Title
Development of a Two-Beam High-Current Ion Accelerator Based on Doppler Effect

Authors
Ivanov, B.
Yegorov, A.M.

Publication Date
1995-03-01

LBL-36841
UC-414

Lawrence Berkeley Laboratory
UNIVERSITY OF CALIFORNIA

Accelerator & Fusion Research Division

Development of a Two-Beam High-Current Ion Accelerator Based on Doppler Effect

B.I. Ivanov and A.M. Yegorov

March 1995

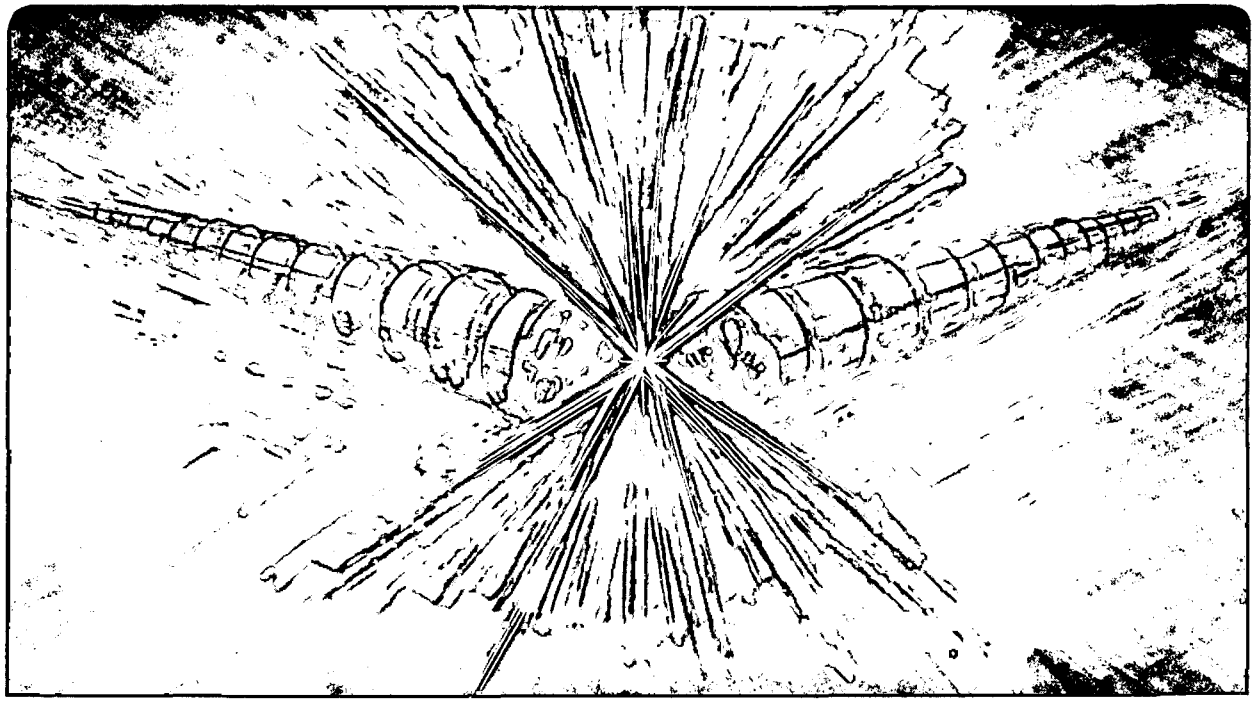

Prepared for the U.S. Department of Energy under Contract Number DE-AC03-76SF00098

DISCLAIMER

LBL-36841
UC-414
CBP Note - 137

Development of a Two-Beam High-Current Ion Accelerator Based on Doppler Effect

B.I. Ivanov and A.M. Yegorov

Center for Beam Physics
Accelerator and Fusion Research Division
Lawrence Berkeley Laboratory
University of California
Berkeley, California 94720

March 1995

This work was supported by the Director, Office of Energy Research, Office of High Energy and Nuclear Physics, Division of High Energy Physics, of the U.S. Department of Energy under Contract No. DE-AC03-76SF00098.

LBL #36841
CBP NOTE# 137

DEVELOPMENT OF A TWO-BEAM HIGH-CURRENT ION ACCELERATOR BASED ON DOPPLER EFFECT

FINAL REPORT (1994)
KHARKOV INSTITUTE OF PHYSICS & TECHNOLOGY
KHARKOV, UKRAINE

PURCHASE ORDER No 4596310
UNIVERSITY OF CALIFORNIA
LAWRENCE BERKELEY LABORATORY
BERKELEY, CALIFORNIA, USA

HEAD OF THE PROJECT B.I. IVANOV

AUTHORIZED BY
INSTITUTE VICE-DIRECTOR A.M. YEGOROV

1. Introduction

This Final Report presents the results of work accomplished in accordance with the Scope of Work to the Purchase Order No 4596310 (Appendix A). The amount of works includes the following items.

1. Start of the manufacture of the Experimental Accelerating Stand (EAS) - the section for proton acceleration from 5 MeV to 8 MeV, in which RF fields are excited by an electron beam at the anomalous Doppler effect.

2. Theoretical investigation and computer simulation of field excitation and ion acceleration in the EAS.

Under item 1, the EAS manufacturing is begun. To present time, a pedestal for the EAS and a stainless steel vacuum chamber for RF resonator are made (length of the chamber is about 180 cm, diameter is about 40 cm); see, accordingly, referense numbers 10 and 9 on the assembly drawing of the EAS in Interim Report, 1993. Besides, parts of the EAS resonator with the acceleration structure are manufactured, and its assembly is begun (see the assembly drawing of the H-type resonator in the Interim Report, 1993).

Under item 2, it is realized three works: calculation of increment and frequency shift of the EAS resonator excited by electron beam, calculation of the solenoid for creation of magnetic field with required spatial distribution, and theoretical investigation and computer simulation of ion acceleration in the EAS.

The first work use the method of perturbation theory developed by J. Slater and modernized by M. Kapchinsky and L. Yudin. In the case of RF field excitation in the EAS resonator by an electron beam under anomalous Doppler effect the small parameter is the relation of plasma frequency of a beam to electron cyclotron frequency. With help of modernized perturbation theory it is possible to calculate and optimize the conditions of RF field excitation in the EAS. In particular, in area of the resonance under anomalous Doppler effect it have been determined the conditions favorable for analysis and functioning of a two-beam ion accelerator (in particularly, the EAS), when RF fields are excited at zero shift of resonator frequency (in known designations these conditions are recorded as Im $\omega > 0$, Re $\omega = 0$). It have been determined the values of the start current, the RF oscillations excitation increment, the frequency shift of the H-type resonator for the main parameters of the EAS.

In second work the question of synthesis of stationary magnetic fields with required dependence on longitudinal coordinate is described. Thus it is used the regularization method developed by A.N. Tikhonov and V.Ya. Arsenin for solution of (so named) incorrect inverse problems. The calculations enabling to create the required distribution of magnetic field in solenoid consisting of separate sections (coils), by variation practically of any parameters of these sections, are conducted. The results of calculations are checked experimentally.

The calculation of a solenoid for creation of a non-uniform resonant magnetic field in the EAS have been accomplished. In this case the conditions of resonance under anomalous Doppler effect is fulfilled on all length of the EAS resonator in spite of the fact that the phase velocity of accelerating wave changes along the EAS (in known notation this condition is recorded as $\omega = k_z(z) \cdot V_0 - \omega_H(z)$).

In third work results of theoretical investigations and computer simulations of ion acceleration in a two-beam electron-ion accelerator are represented (with taking into account of the main EAS parameters). (Theoretical investigations and computer simulations of RF fields excitation under unomalous Doppler effect conditions, with regarding the EAS, are described in the Report-1993, and in 1-st part of this Report). Detailed study of ion acceleration dynamics and its radial focusing have been realized. Computer simulations of ion acceleration and focusing have been accomplished for wide set of parameters including the main EAS parameters.

The Report contains 34 pages, 14 figures, 16 references.

2. Start of Experimental Accelerating Stand Manufacturing

In 1994 it is started the manufacture of the Experimental Accelerating Stand (EAS) - the section for proton acceleration from 5 MeV to 8 MeV, in which RF fields are excited by an intense electron beam under anomalous Doppler effect conditions.

To present time a stainless steel vacuum chamber for the EAS RF-resonator (length of the chamber is about 180 cm, diameter is about 40 cm), and a pedestal for the EAS have been made (see, accordingly, referense numbers 9 and 10 in the assembly drawing of the EAS in the Interim Report, 1993).

Besides, parts (workpieces) of the EAS resonator with the acceleration structure have been manufactured, and its assembly is begun (for reference, see the assembly drawing of the H-type resonator in the Interim Report, 1993).

On the next page it is represented the view of the one-half of the EAS resonator (top) in the assembly process, and parts of the EAS accelerating structure (bottom). A scale of the bottom photograph is represented by a vernier caliper with the length of 25 cm (see Fig.1).

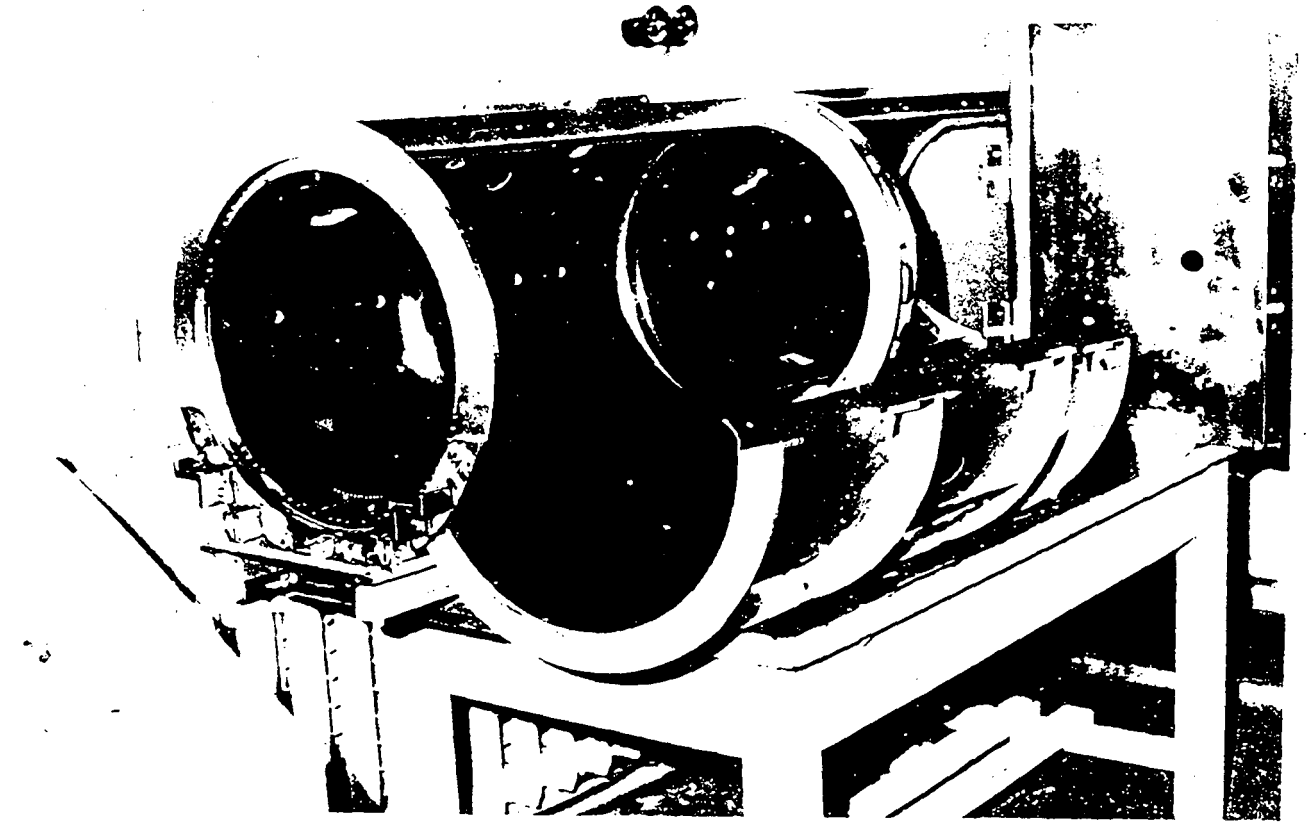

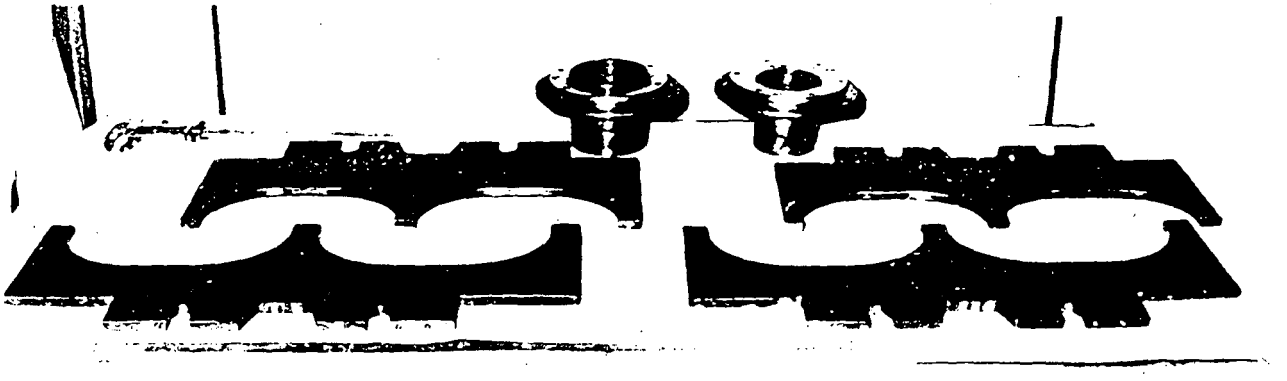

Fig. 1

3. Calculation of Frequency Shift and Increment for the EAS Resonator Exciting due to Anomalous Doppler Effect (Non-Uniform Case)

For development of different kinds of ion acceleration by means of electromagnetic fields of cavity's oscillation excited by electron beams it is very important an investigation of such problem as cavity's frequency shift that is caused by electron beam that is passing through the cavity. If an electron beam is intensive enough then the frequency shift may be rather big and it must be taken into account. In these conditions it is useful to have zero frequency shift because we may do synchronism tuning as in the case of "cold" structure.

1. For frequency shifts calculating we will use the Slater's formula:

$$\delta\omega = -\frac{i}{4W_c}\int \bar{j}\bar{E}^* dV \ , \qquad (1)$$

where $\delta\omega$ is a frequency shift, W_c - energy of cavity oscillation, $\bar{E}$ - electric field of oscillation, $\bar{j}$ - RF current induced in the beam by electromagnetic field of cavity, star means complex conjugation, all values here depend from time as $\exp(-i\omega t)$. Integration must be done upon the volume of the cavity.

In the first order of perturbation theory values W_c and $\bar{E}(\bar{r})$ must be treated as characteristics of undisturbed oscillation of the cavity. Such "cold" characteristics are usually known after tests and measures of cavity before it would be put to the experimental device.

Formula (1) is widely used; for calculating of RF current $\bar{j}(\bar{r},\omega)$ induced in electron beam by known field $\bar{E}(\bar{r},\omega)$ of a cavity they tried to solve differential equations of particles' motion in this field. For the cavity of complex configuration such problem is rather difficult due to complicated view of function $\bar{E}(\bar{r},\omega)$.

We are supposing another procedure. Differential equations of particles' motion may be solved in general form and reduced to calculation of definite integrals. For the case of the beam focused by spatially uniform magnetic field this procedure was described in [1, 2].

In the frame where electron beam is in rest the connection between RF electric field and RF current induced by it may be written as follows:

$$\bar{j}'(\bar{r}) = -\frac{i\omega'}{4\pi}\int \hat{\Phi}(\bar{r},\bar{\rho})\bar{E}'(\bar{\rho})d\rho \ , \qquad (2)$$

where stroke marks values in the rest frame of the beam, $\hat{\Phi}(\bar{r},\bar{\rho})$ - tensor function of response. It is important to note that this function depends only from beam characteristics and static fields by which the electron beam is focusing and doesn't depend from RF fields of cavity's oscillation. For Lorentz's transformations where one frame is moving onward to the other all components of this tensor-function behave as relativistic scalars.

For the case of the beam which particles are not rotate in the absence of RF field (such beams are produced from magnetized cathodes) the spatial dispersion vanishes in directions that are transverse to magnetic field and beam velocity so we obtain

$$\bar{j}'(\bar{r}_\perp, z) = -\frac{i\omega'}{4\pi}\int \hat{\Phi}(z,\varsigma)\bar{E}'(r_\perp,\varsigma)d\varsigma \ . \qquad (3)$$

Because of causality principle bounds in the integral are $-\infty$ and z or in the case of cavity we must integrate from the beginning of the cavity till the point where $\bar{j}$ is calculating.

In laboratory frame relation (1) goes to the next:

$$\delta\omega = -\frac{\omega}{16\pi W_c}\int d\bar{r}_\perp \int_0^L \left\{ \gamma^2 \bar{K}^*(z)\int_0^z \hat{\Phi}_\perp(z,\varsigma)\bar{K}(\varsigma)d\varsigma + E_z^*(z)\int_0^z \Phi_{\parallel}(z,\varsigma)E_z(\varsigma)d\varsigma \right\} dz \quad , (4)$$

where γ - relativistic beam factor, $\bar{K} = \bar{E}_\perp + \frac{1}{c}\left[\vec{u}, \bar{B}_\perp\right]$ - Lorentz's field combination, $\vec{u}$ - beam velocity, c - light speed, 0 and L - coordinates of cavity ends, $\hat{\Phi}_\perp(z,\varsigma)$ and $\Phi_{\parallel}(z,\zeta)$ - transverse and longitudinal components of tensor response function.

As we are interesting in cyclotron resonances we must take into account only first summand in (4) which is responsible for transverse beam-field interactions. Further, in the case of axe-symmetrical oscillation we must consider only E_r and B_θ field components. Formula (4) reduces to

$$\delta\omega = -\frac{\omega\gamma^2}{16\pi W_c}\int d\vec{r}_\perp \int_0^L \gamma^2 K_r{}^*(z)\int_0^z \Phi_{rr}(z,\zeta)K_r(\zeta)d\zeta\, dz \quad , \qquad (5)$$

where γ is relativistic factor.

For the beam in spatially uniform longitudinal magnetic field function of response was

$$\Phi_{rr}(z,\zeta) = \frac{i\omega_b^2}{16\pi\Omega u}\left[\exp\left(i\frac{\omega-\Omega}{u}(z-\zeta)\right) - \exp\left(i\frac{\omega+\Omega}{u}(z-\zeta)\right)\right] .$$

Now in non-uniform magnetic field it is more complicated and may be found by method from [3]. It is equal to

$$\Phi_{rr}(z,\zeta) = \frac{i\omega_b^2}{2\gamma^2\Omega_i u}\left(\frac{\Omega(z)}{\Omega(\zeta)}\right)^{1/2}\left[\exp\int_\zeta^z\left(i\frac{\omega-\Omega(s)}{u}ds\right) - \exp\int_\zeta^z\left(i\frac{\omega+\Omega(s)}{u}ds\right)\right] , \qquad (6)$$

where $\Omega(z) = e_0 H(z)/\gamma m_0 c$ - cyclotron frequency, e_0 - electron charge, m_0 - electron mass, $H(z)$ - static longitudinal magnetic field, $\omega_b = \left(4\pi n_b e_0^2/m_0\gamma\right)^{1/2}$ - plasma frequency of electron beam in the entrance of the cavity, Ω_i - initial value of cyclotron frequency. Relation (5) may be rewritten as the difference

$$\delta\omega = \Psi_- - \Psi_+ \quad , \qquad (7)$$

where

$$\Psi_\pm = \frac{-i\omega}{32\pi u W_c\Omega_i}\int\omega_b^2\int_0^L K_r^*(z)\int_0^z\left(\frac{\Omega(z)}{\Omega(\zeta)}\right)^{1/2}\exp\int_\zeta^z\left(i\frac{\omega\pm\Omega}{u}ds\right)K_r(\zeta)d\zeta dz d\vec{r}_\perp . \qquad (8)$$

In (7) term Ψ_+ describes an interaction between cavity's oscillation and slow cyclotron wave of electron beam while Ψ_- is responsible for excitation of fast cyclotron wave.

For EAS parameters where energy of ions must increase

$$W(z) = W_i + \left(W_f - W_i\right)\frac{z}{L} \qquad (9)$$

from W_i in the entrance to W_f in the exit of the cavity cyclotron frequency must decrease with the length

$$\Omega(z) = \omega\left[\frac{u}{c}\left(\frac{W_p}{2W(z)}\right)^{1/2} - 1\right] \quad , \qquad (10)$$

integral from it is equal to

$$\int_0^z \Omega(s)ds = \omega\left[\frac{uL(2W_p)^{1/2}}{c(W_f - W_i)}\left(\sqrt{W(z)} - \sqrt{W_i}\right) - z\right] \quad . \qquad (11)$$

Here W_p = 940 MeV - proton rest energy.

While calculating frequency shifts (and increments) by means of perturbation theory in the first order we may use non-disturbed fields of cold structure. As small parameter of expansion here appears ω_b^2/Ω^2 . Region of parameters $\omega_b \sim \omega$ corresponding to dense beams is included by this approximation.

Longitudinal component of RF electric field in EAS's cavity is equal to

$$E_z(r,z) = A_j I_0(\kappa_j r)\cos k_j(z - z_j) \quad , \qquad (12)$$

where j - number of the gap that is nearest to point with coordinate z , z_j - center of this gap (in EAS's structure "gap" includes the gap itself and halves of neighboring drift tubes),

$$k_j = k(z_j) = \frac{\omega}{c}\left[W_p \Big/ 2W(z_j)\right]^{1/2} \quad , \qquad (13)$$

longitudinal wave number in vicinity of the gap, $\kappa_j = \left(\omega^2/c^2 + k_j^2\right)^{1/2}$ - transverse wave number, A_j - complex amplitude, $I_0(x)$ - modified Bessel's function. Transverse field components are

$$E_r(r,z) = A_j \frac{k_j}{\kappa_j} I_1(\kappa_j r)\sin k_j(z - z_j)$$

and

$$B_\theta(r,z) = \frac{i\omega}{c\kappa_j} A_j I_1(\kappa_j r)\cos k_j(z - z_j) \quad ,$$

Lorentz's field combination is

$$K_r(r,z) = A_j \frac{1}{\kappa_j} I_1(\kappa_j r)\left[k_j \sin k_j(z-z_j) + i\frac{u\omega}{c^2}\cos k_j(z-z_j)\right] \qquad (14)$$

Formulas (9) - (14) must be substituted in (8) and (7) for numerical calculation of frequency shift.

2. Direct calculation by formulas (7) and (8) is close to impossible. The cause is the double integral in (8) by longitudinal coordinate. Restrictions on computer's memory don't permit to choose sufficiently small step of integration so numerical error is very big here. For getting approximate result we may choose a model where magnetic field changes step by step on every gap of resonator. Since number of the gaps is rather big such approximation is not very rough. Now we can change an integrals by sums, each summand will be the meaning of the integral on one gap. One more approximation: beam radius $a(z)$ is small by comparison with the length of the gaps so we may write in (14) $\frac{1}{2}\kappa_j r$ instead of $I_1(\kappa_j r)$.

Expression (8) now looks out

$$\Psi_{\pm} = \frac{-i\omega c^3 a_i^2 \Omega_i |Y|^2 J}{64u^2\gamma W_c J_0} \sum_{j=1}^{N} \int_{b_{j-1}}^{b_j} \frac{\alpha_j^* \varphi_j^*(z)}{\Omega_j^{3/2}} \exp\left[\frac{i}{u}\int_0^z (\omega \pm \Omega(s))ds\right] \times \qquad (15)$$

$$\left\{ \sum_{k=1}^{j-1} \int_{b_{k-1}}^{b_k} \frac{\alpha_k \varphi_k(\zeta)}{\sqrt{\Omega_k}} \exp\left[-\frac{i}{u}\int_0^\zeta (\omega \pm \Omega(s))ds\right] d\zeta + \int_{b_{j-1}}^{z} \frac{\alpha_j \varphi_j(\zeta)}{\sqrt{\Omega_j}} \exp\left[-\frac{i}{u}\int_0^\zeta (\omega \pm \Omega(s))ds\right] d\zeta \right\} dz$$

where N is number of the gaps, Ω_j is the value of cyclotron frequency along the gap with number j, b_{j-1} and b_j are coordinates of the beginning and the end of the j-th gap, Y is field amplitude in the middle of the cavity and α_j is relative field amplitude in each gap. Function $\varphi_j(z) = k_j \sin k_j(z-z_j) + \frac{iu\omega}{c^2}\cos k_j(z-z_j)$ represents distribution of the field upon each gap. In (15) we've account already that beam radius varies by the law $a(z) = a_i\sqrt{\Omega_i/\Omega(z)}$ and made an integration on transverse coordinate r. So J is the beam current and J_0 = 17 kA is Alfven current. Each integral in (15) can be calculated analytically. Ultimate expression is hard to see but easy for calculate:

$$\Psi_{\pm} = \frac{-i\omega c^3 a_i^2 \Omega_i |Y|^2 J}{64u^2\gamma W_c J_0} \sum_{j=1}^{N} \chi_j \quad , \qquad (16)$$

where

$$\chi_j = \frac{\alpha_j^*}{\Omega_j^{3/2}} k_j u \frac{\omega\beta^2 - (\omega \pm \Omega_j)}{k_j^2 u^2 - (\omega \pm \Omega_j)^2}\left[1 + \exp\left(i\pi \frac{\omega \pm \Omega_j}{k_j u}\right)\right]\exp\left(i\pi \sum_{l=1}^{j-1} \frac{\omega \pm \Omega_l}{k_l u}\right) \times$$

$$\times \sum_{k=1}^{j-1}\left\{\frac{\alpha_k}{\Omega_k^{1/2}} k_k u \frac{\omega\beta^2 - (\omega \pm \Omega_k)}{k_j^2 u^2 - (\omega \pm \Omega_k)^2}\left[1 + \exp\left(-i\pi \frac{\omega \pm \Omega_k}{k_k u}\right)\right]\exp\left(i\pi \sum_{l=1}^{k-1} \frac{\omega \pm \Omega_l}{k_l u}\right) + \right.$$

$$+ \frac{|\alpha_j|^2}{\Omega_j^2}\left\{2\left[k_j u \frac{\omega\beta^2 - (\omega \pm \Omega_j)}{k_j^2 u^2 - (\omega \pm \Omega_j)^2}\right]^2\left[1 + \exp\left(i\pi \frac{\omega \pm \Omega_j}{k_j u}\right)\right] - \right. \qquad (17)$$

$$\left.\left. - \frac{i\pi u}{k_j} \frac{(\omega \pm \Omega_j)\left(\frac{\beta^2\omega^2}{c^2} + k_j^2\right) - 2\omega\beta^2 k_j^2}{k_j^2 u^2 - (\omega \pm \Omega_j)^2}\right\}\right\},$$

and $\beta = u/c$ - relative beam velocity.

Usually it is convenient to express a frequency shift through form-factor F :

$$\delta\omega = \frac{1}{2}\omega\frac{\omega_b^2}{\omega^2}F \qquad (18)$$

and to use instead of the ratio $|Y|^2/W_c$ two other characteristics of the cavity: shunt resistance R_{sh} and quality factor Q . For the cavity with proper fields like (12) we can write

$$\frac{|Y|^2}{W_c} = \frac{\omega}{2}\frac{R_{sh}}{Q}\left(\sum_{j=1}^{N}\frac{|\alpha_j|}{k_j}\right)^{-2} \qquad (19)$$

Form-factor also consists from two summands

$$F = F_- - F_+ \qquad (20)$$

In dimensionless form they are:

$$F_{\pm} = -\frac{i}{256}\frac{\omega}{\Omega_i}\left(\frac{\omega a_i}{c}\right)^2 \frac{1}{\beta}\frac{cR_{sh}}{Q}\left(\sum_{j=1}^{N}\frac{|\alpha_j|}{k_j a_i}\right)^{-2}\sum_{j=1}^{N}(\Omega_i^2\chi_j) \quad , \qquad (21)$$

where χ_j are given by (17).

3. Numerical calculations based on formulas (20) and (21) with parameters for EAS device are shown below on Fig. 2.

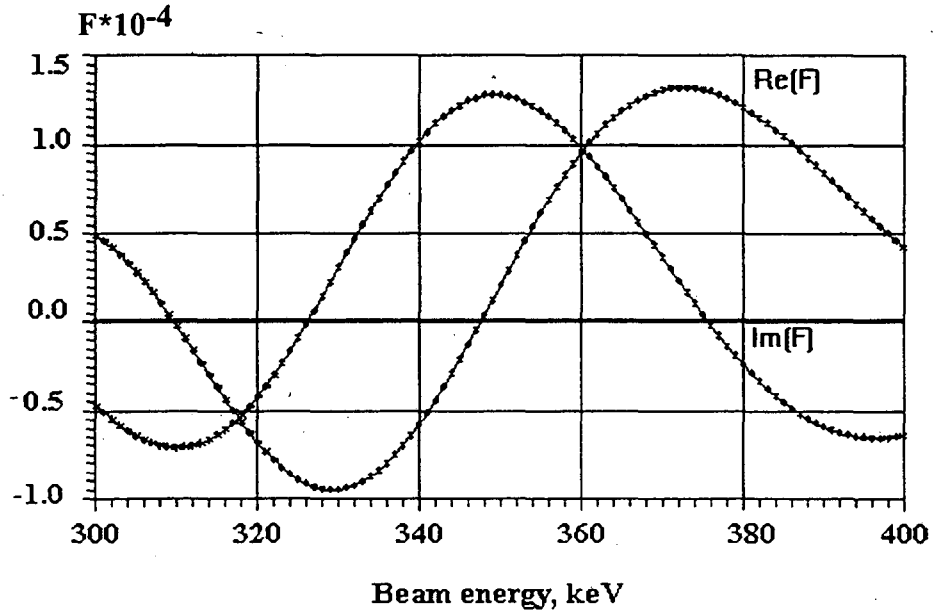

Fig. 2. Real and imaginary parts of form-factor vs. beam energy.

Maximum increment corresponding Im(F) = $1.3\cdot10^{-4}$ is equal to $1.3\cdot10^{6}$ sec^{-1} for electron beam current 200 A. Taking into account natural damping due to finite cavity's quality factor leads to diminishing these values on 22%. Start current of EAS resonator is 37 A.

4. Calculation of a Solenoid for Creation of Magnetic Field With a Required Spatial Distribution

1. For development of the two-beam ion accelerator we need to produce an axially symmetrical magnetic field with a required longitudinal dependence. This field may be formed by a sectionalized solenoid. Magnetic field created by sections (coils) depends on their parameters, then by calculations and variations of these parameters, one can produce a required spatial distribution. Solution of this problem is not easy; in this case the regularization method of A.N. Tikhonov [4] may be used. In previous papers [5-8] calculations were carried out in which magnetic field linearly depends on sections' parameters. As a rule, this linear parameter was a magnitude of current in each section. Unfortunately, in this case it is difficult to reach optimum loading for each section. Then power supply of a solenoid would be rather complicated.

2. In this work more general solution is given in which a nonlinear parameter ($N_1, N_2,...N_n$) of sections is determined. It can be, for example, thickness of winding, length of section, inner radius, etc., i.e. sizes, on which the intensity of field depends, generally speaking, nonlinearly (see also Ref [11]).

We consider the sectionalized solenoid, consisting of n coaxial sections of arbitrary winding sectional view. Let the intensity of field, created by i-th section in point z, is described by function $H_i\ (N_i, z)$, and intensity of field, which is necessary to be created on axis of solenoid on interval $[a, b]$, - by function $B(z)$. Then

$$\sum_{i=1}^{n} H_i(N_i, z) = B(z) \tag{1}$$

and task is reduced to finding of vector $N=(N_1, N_2,...N_n)$. As far as the equation (1), in general case,has not exact solutions,then speech goes about finding a quasi-solution minimizing smoothing functional [4]

$$F(N_1,...,N_n,\beta) = \int_a^b \alpha(z)\left[\sum_{i=1}^{n} H_i(N_i,z) - B(z)\right]^2 dz + \beta \sum_{j=1}^{n} N_j^2, \tag{2}$$

where $\alpha(z)$ is a weight function, β is a parameter of regularization. The weight function $\alpha(z)$ is entered for improvement of approximation of function $B(z)$ on ends of interval $[a, b]$.

The conditions of minimum of functional (2)

$$\frac{\partial\ F(N_1,...,N_n,\beta)}{\partial\ N_k} = 0$$

give the system of nonlinear equations

$$\int_a^b \alpha(z)\left[\sum_{i=1}^{n} H_i(N_i,z) - B(z)\right]\frac{\partial\ H_k(N_k,z)}{\partial\ N_k} dz + \beta N_k = 0 \tag{3}$$

which is possible to be solved by one of known methods (see, for example, [9]).

For solution of system (3) by Newton method we expand the function $H_i\ (N_i, z)$ in Taylor series in point N_i^{l-1} and are limited by linear terms of series. We have

$$\sum_{i=1}^{n} A_{ik} N_i^l + \beta N_k^l = C_k , \tag{4}$$

where

$$A_{ik} = \int_a^b \alpha(z) \left. \frac{\partial H_i(N_i,z)}{\partial N_i} \right|_{N_i = N_i^{l-1}} \left. \frac{\partial H_k(N_k,z)}{\partial N_k} \right|_{N_k = N_k^{l-1}} dz , \tag{5}$$

$$C_k = \int_a^b \alpha(z) \left\{ B(z) - \sum_{i=1}^{n} \left[H_i(N_i^{l-1},z) - \left. \frac{\partial H_i(N_i,z)}{\partial N_i} \right|_{N_i = N_i^{l-1}} N_i^{l-1} \right] \right\} \times$$

$$\times \left. \frac{\partial H_k(N_k,z)}{\partial N_k} \right|_{N_k = N_k^{l-1}} dz \tag{6}$$

N_i^l - significance of required vector on l-th iteration. The parameter of regularization β is possible to be determined from equation

$$\int_a^b \alpha(z) \left[H(N_1^0,\ldots,N_n^0,z) - B(z) \right]^2 dz + \beta \sum_{j=1}^{n} N_j^{02} = \delta^2 \tag{7}$$

where δ - the relative error; the vector $N^0 = (N_1^0,\ldots,N_n^0)$ satisfies to set of equations (3), if the functional $H(N_1,\ldots,N_n,z) = \sum_{i=1}^{n} H_i(N_i,z)$ is convex [4].

In case of arbitrary nonlinear functional $H(N_1,\ldots, N_n, z)$ it is possible to use alternative way of choosing of regularization parameter [10].

The weight function $\alpha(z)$ should have rises on ends of the interval $[a, b]$, because approximation of a field grows worse there. But in elementary case the weight function may be simply a constant.

3. The algorithm (4)-(6) was realized on a computer for the case of a solenoid consisting of sections with a rectangular sectional view of winding. Then approximation functions $H_i(N_i, z)$ have the form:

$$H_i(z) = \frac{2\pi \cdot J_i \delta_i}{c} \left[(z-\xi_i) \ln \frac{R_i + \sqrt{R_i^2 + (z-\xi_i)^2}}{r_i + \sqrt{r_i^2 + (z-\xi_i)^2}} - \right.$$

$$\left. -(z-a_i-\xi_i) \ln \frac{R_i + \sqrt{R_i^2 + (z-a_i-\xi_i)^2}}{r_i + \sqrt{r_i^2 + (z-a_i-\xi_i)^2}} \right], \text{ Oe}$$

where J_i-current density, Gauss units; δ_i-coefficient of filling; ξ_i-coordinate of section beginning, cm; r_i-inner radius of section, cm; R_i-outer radius of section, cm; a_i-length of section, cm; c-velocity of light, cm/s.

For values be found three kinds of section parameters were accepted: the thickness of winding $d_i = R_i - r_i$, length of section a_i and coordinate of section ξ_i. The density of current in all sections is identical, that excludes overloading of the end-sections. In this case the wire consumption is more rational, and power supply is simple since all sections are connected in series. All this in final result minimazes dimensions, weight and cost of solenoid.

As a weight function $\alpha(z)$ it is used the following one:

$$\alpha(z) = 1 + \left(\frac{z-e}{d}\right)^4, \qquad (z=[0,b],\ e=0,5b,\ d=0,25b)$$

The results of calculations (for the case of winding thickness variation) are adduced on Fig. 1. Here the function $B(z)$ is designated by dashed line (this is a field required), and

$H(N_1^0,\ldots,N_n^0,z) = \sum_{i=1}^{n} H_i(N_i,z)$ is designated by continuous line (this is a field created on axis of a sectionalized solenoid). As is visible, the good concurrence of these functions on all interval $[0, b]$, b=140 cm, is observed.

For check of the method described in this work the solenoid consisting of nine identical coils was made, and required configuration of magnetic field was reached by calculated mutual arrangement of these coils. The results of measurements of magnetic field are submitted on Fig. 2 where the shaped line corresponds to the calculations, and the continuous one - to the experiment. The maximal error on the working interval from 0 to 80 cm (caused basically by not very good accuracy of coils manufacturing and field measurements) does not exceed 5 %.

By this method the calculations of a solenoid for creation of a non-uniform resonant magnetic field in the EAS are accomplished. In this case the resonance condition under anomalous Doppler effect is realized on all length of EAS resonator in spite of the fact that the phase velocity of accelerating wave changes along the EAS. For calculation of solenoid the EAS parameters adduced in Tables 1 and 2 of Final Report, 1993, are used. Results of solenoid calculations are adduced in Table 1 of this Report. Besides the large coils of solenoid (No 1-14, 17) the small coils which focus an electronic beam on way from a gun to the resonator (No 15-16) are discounted also. The deviation of created magnetic field from required one [determined by condition $\omega = k_z(z)\cdot V_e - \omega_H(z)$] on all length of resonator does not exceed 1 %.

Table 1

coil number	number of turns in coil	wire section, mm^2	space factor of a winding	coordinate of coil, cm	length, cm	inner radius, cm	current, A	thickness of winding, cm	resistance, Ohm	Power, W	wire length, m	weight, kg
1	76	56.0	0.8	-1.40	5.8	39.0	140.0	9.23	$6.18 \cdot 10^{-2}$	1210	207	103
2	65	56.0	0.8	10.81	5.8	39.0	140.0	7.90	$5.21 \cdot 10^{-2}$	1020	174	86.8
3	40	56.0	0.8	21.44	5.8	39.0	140.0	4.87	$3.09 \cdot 10^{-2}$	606	103	51.5
4	22	56.0	0.8	32.33	5.8	39.0	140.0	2.64	$1.66 \cdot 10^{-2}$	325	55.4	27.6
5	30	56.0	0.8	43.47	5.8	39.0	140.0	3.66	$2.29 \cdot 10^{-2}$	448	76.5	38.1
6	38	56.0	0.8	54.87	5.8	39.0	140.0	4.60	$2.93 \cdot 10^{-2}$	574	98.0	48.8
7	39	56.0	0.8	66.53	5.8	39.0	140.0	4.71	$3.01 \cdot 10^{-2}$	590	101	50.2
8	39	56.0	0.8	78.45	5.8	39.0	140.0	4.65	$3.01 \cdot 10^{-2}$	590	101	50.2
9	40	56.0	0.8	90.62	5.8	39.0	140.0	4.78	$3.09 \cdot 10^{-2}$	606	103	51.5
10	35	56.0	0.8	103.05	5.8	39.0	140.0	4.27	$2.69 \cdot 10^{-2}$	526	89.9	44.8
11	21	56.0	0.8	115.74	5.8	39.0	140.0	2.52	$1.58 \cdot 10^{-2}$	309	52.8	26.3
12	31	56.0	0.8	128.68	5.8	39.0	140.0	3.76	$2.36 \cdot 10^{-2}$	463	79.2	39.4
13	66	56.0	0.8	141.88	5.8	39.0	140.0	8.01	$5.30 \cdot 10^{-2}$	1040	177	88.3
14	78	56.0	0.8	155.54	5.8	39.0	140.0	9.42	$6.37 \cdot 10^{-2}$	1250	213	106
15	200	4.91	0.7	-50.0	6.0	5.3	12.27	2.34	$2.27 \cdot 10^{-2}$	34.3	66.7	2.91
16	380	4.91	0.7	-44.0	19.0	9.5	12.27	1.40	$7.74 \cdot 10^{-1}$	117	227	9.91
17	80	56.0	0.8	-14.0	5.8	39.0	140.0	9.66	$5.86 \cdot 10^{-2}$	1150	196	97.7

Resistance of the solenoid	$0.155 \cdot 10^{1}$	Ohm
Power of the solenoid	$0.109 \cdot 10^{5}$	W
Weight of the solenoid	$0.923 \cdot 10^{3}$	kg

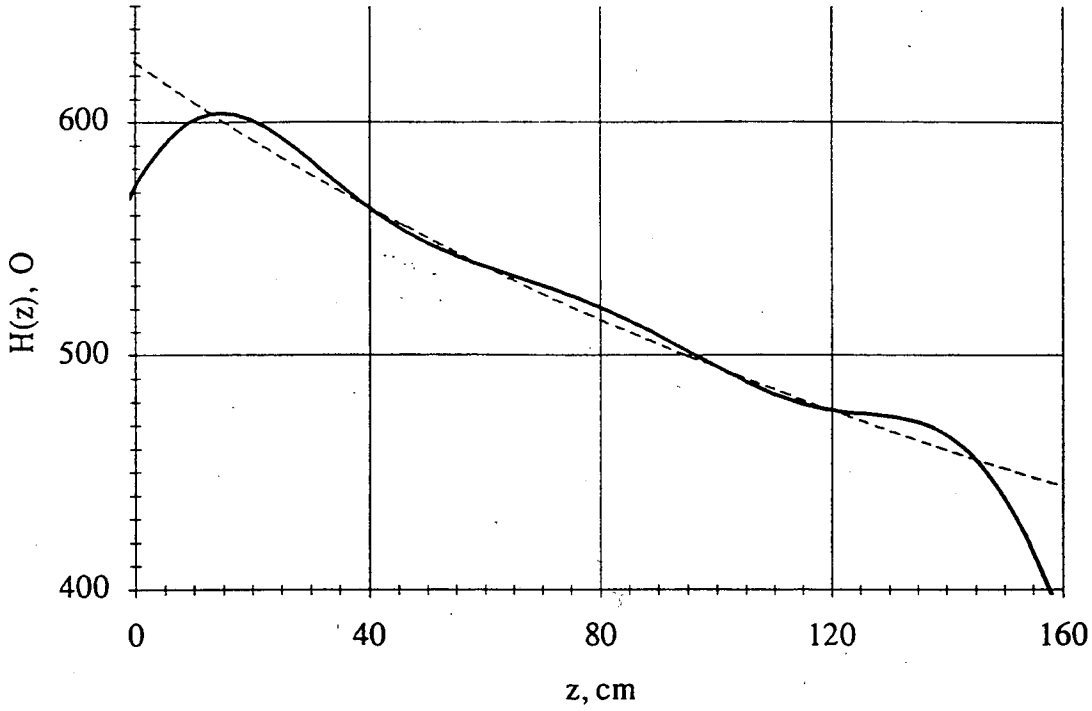

Fig. 3. Longitudinal magnetic field (Oe) versus longitudinal coordinate (cm)

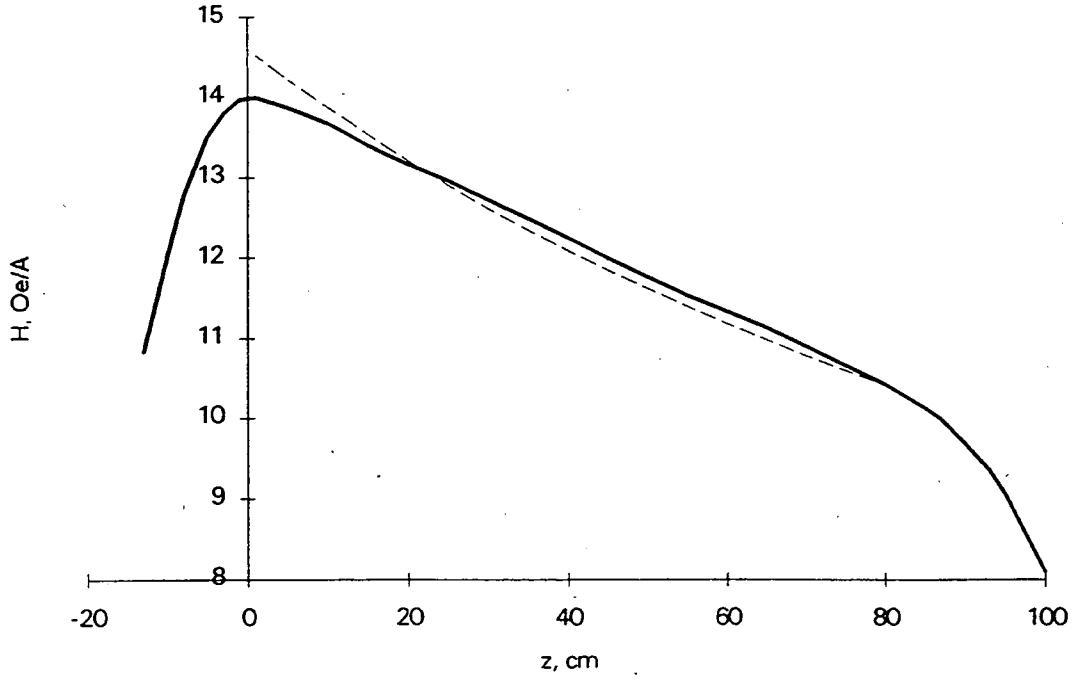

Fig. 4. Relation of magnetic field (Oe) to solenoid current (A) versus longitudinal coordinate (cm)

5. Theoretical Investigation and Computer Simulation of Ion Acceleration in a Two-Beam Electron-Ion Accelerator (with Regarding the EAS Parameters)

In the previous Report (1993), and in first part of this Report we have investigated the problem of accelerating RF-fields excitation in H-type resonator by high current electron beam under anomalous Doppler effect conditions to ground future experiments on the EAS installation. The perturbation theory was used for obtaining of nonlinear self consistent set of equations of wave excitation even for the beam of sufficiently big density (ω–ω_b) if the following condition is fulfilled:

$$\frac{\delta k}{k_z} = \frac{\omega_{b\perp}}{k_z V_0}\left(1 - \beta_{ph}\beta_0\right)\sqrt{\frac{\omega}{2\omega_H}\mathrm{I}_1\left(k_\perp \bar{r}_b\right)} << 1 \qquad (1)$$

The expression (1) corresponds to the small ratio of spatial growth rate δk to wave number (k_z); it is conditioned by small geometric factor determined by the negligible volume that electron beam occupied in the resonator of H-type (designations to expression (1) are listed below).

In the present Report the dynamics of accelerated ion in the field of already excited wave is considered. In this case an essential feature is the topography changing in the electron beam body which can radically modify the radial - phase dynamics of accelerated ions. It was supposed that the presence of electron beam in H-type resonator lead to negligible changing of dispersion characteristic of the excited wave. We take into account the topography modification by means of changing of transversal wave number for the wave excited in H-type resonator at anomalous Doppler effect (ADE). Besides the influence of space charge forces of the electron beam on ions dynamics will be considered.

Let us consider excitation of H-type resonator placed in an external magnetic field H_0 by an electron beam of density n_0 under the conditions of ADE:

$$\omega = k_z V_0 - \omega_H \qquad (2)$$

Here ω is the frequency of the excited wave; k_z is the wave number corresponding to π - mode: $k_z=2\pi/L$; L is the length of the structure period; V_0 is the velocity of beam electrons; $\omega_H = eH_0/mc\gamma_0$ is the cyclotron frequency, γ_0 is relativistic factor of beam electrons.

The components of the electric field of the excited wave can be taken in the form:
in the vacuum region ($r_b<r<r_d$, r_d - drift tube radius, r_b - beam radius.) (see , e.g. [12]):

$$E_z = E_0 I_0\left(k_\perp r\right)\cos\Phi,\ E_r = \frac{k_z}{k_\perp} E_0 I_1\left(k_\perp r\right)\sin\Phi \qquad (3)$$

in the electron beam region ($0<r< r_b$) (see , e.g. [13]):

$$E_z = E_0\, \mathrm{J}_0(\kappa r)\cos\Phi,\ E_r = \frac{\varepsilon_\parallel}{\varepsilon_\perp} E_0\, \mathrm{J}_1(\kappa r)\sin\Phi, \qquad (4)$$

where E_0 - field amplitude on the axis; $\Phi \equiv \omega\left(\int \frac{dz}{V_{ph}} - t\right)$ - ion phase taken from the maximum of the accelerating wave; $V_{ph} = \omega/k_z(z)$ - changing wave number ($V_{ph}(z=0) = V_{ph0} = \omega/k_0$); J_0, J_1, I_0, I_1 - usual and modified Bessel functions, and

$$k_\perp \approx k_z,\ \kappa = \sqrt{-\varepsilon_\parallel/\varepsilon_\perp}\,k_z,\ \varepsilon_\parallel = 1 - \frac{\omega_{b\parallel}^2}{\left(\omega - k_z V_0\right)^2},\ \varepsilon_\perp = 1 - \frac{\omega_{b\perp}^2}{\left(\omega - k_z V_0\right)^2 - \omega_H^2}, \qquad (5)$$

$\omega_{b\perp}^2 = 4\pi n_0 e^2/m\gamma_0$, $\omega_{b\parallel} = \omega_{b\perp}/\gamma_0$.

Suppose that ions of initial energy W_{i0} are injected into a resonator along the axis. Acceleration process using the motion equations of ions in the electric fields (3), (4) is investigated. Besides, we take into account an influence of electron beam space charge on ions radial oscillations.

By introducing of dimentionless variables:

$$\varsigma = k_0 z,\ \rho = k_0 r,\ \rho_b = k_0 r_b,\ \varepsilon_0 = \frac{eE_0}{m_i k_0 V_{ph0}^2},\ \varepsilon_1 = \varepsilon_0 \mathrm{J}_0\left(\frac{\kappa}{k_0}\rho_b\right)\Big/\mathrm{I}_0\left(\frac{V_{ph0}}{V_{ph}}\rho_b\right) \quad (6)$$

one can obtain the following set of equations (in other cases analogous equations were investigated in Ref. [14, 15]):

for $0<r<r_b$

$$\frac{d^2\Phi}{d\varsigma^2} = \varepsilon_0\left[\frac{V_{ph0}}{V_{ph}(\varsigma)} - \frac{d\Phi}{d\varsigma}\right]^3 \mathrm{J}_0\left(\frac{\kappa}{k_0}\rho\right)\cos\Phi - \frac{V_{ph0}}{V_{ph}^2(\varsigma)}\frac{dV_{ph}(\varsigma)}{d\varsigma} \quad (7a)$$

$$\frac{d^2\rho}{d\varsigma^2} = -\varepsilon_0\left[\frac{V_{ph0}}{V_{ph}(\varsigma)} - \frac{d\Phi}{d\varsigma}\right]^2\left[\frac{d\rho}{d\varsigma}\mathrm{J}_0\left(\frac{\kappa}{k_0}\rho\right)\cos\Phi + \frac{\kappa}{k_0}\mathrm{J}_1\left(\frac{\kappa}{k_0}\rho\right)\sin\Phi + \nu\left(1 - \frac{n_i}{n_e}\right)\rho\right] \quad (7b)$$

for $r_b<r<r_d$

$$\frac{d^2\Phi}{d\varsigma^2} = \varepsilon_1\left[\frac{V_{pho}}{V_{ph}(\varsigma)} - \frac{d\Phi}{d\varsigma}\right]^3 \mathrm{I}_0\left(\frac{V_{pho}}{V_{ph}}\rho\right)\cos\Phi - \frac{V_{pho}}{V_{ph}^2(\varsigma)}\frac{dV_{ph}(\varsigma)}{d\varsigma} \quad (8a)$$

$$\frac{d^2\rho}{d\varsigma^2} = -\varepsilon_1\left[\frac{V_{ph0}}{V_{ph}(\varsigma)} - \frac{d\Phi}{d\varsigma}\right]^2\left[\frac{d\rho}{d\varsigma}\mathrm{I}_0\left(\frac{V_{ph0}}{V_{ph}}\rho\right)\cos\Phi - \mathrm{I}_1\left(\frac{V_{ph0}}{V_{ph}}\rho\right)\sin\Phi + \nu\left(1 - \frac{n_i}{n_e}\right)\frac{\rho_b^2}{\rho}\right] \quad (8b)$$

The last expression in (6) is obtained to satisfy the continuity of the longitudinal components of the electric field on the vacuum-beam boundary $r=r_b$.

The last terms in the right parts of the equations (7b) and (8b) describe radial oscillations of ions in the volume charge fields of the electron beam compensated partially by ion charge. In the most cases, including beams parameters of experiments on EAS one can supposed $n_i<<n_b$.

As it follows from equations (7), (8) there are two qualitatively various cases of ion acceleration and radial focusing in dependence of beam parameters. So, as it was mentioned above, for negligible small beam density or essentially detuning of cyclotron resonance on ADE (and, then, for $\varepsilon_\perp>0$) the radial structure of accelerating field is similar to vacuum one, i.e. electric field increases with radius growth. As it well known in this case there is not existed simultaneously radial and phase stability of accelerated particles.

In other case ($\varepsilon_\perp<0$), near Doppler shifted cyclotron resonance (anomalous and normal Doppler effects), and when density of e-beam is high enough to change radial topography of accelerating field in its region near the axis, the maximum value of electric field E_z is on the beam

axis and it reduces gradually to the beam boundary. Naturally there is the possibility of radial-phase stability for ions, accelerated by such fields.

For the first (beam non-sufficient) case the set of ion motion equations can be represented in the following form:

$$\frac{d^2\Phi}{d\varsigma^2} = \varepsilon_0 \left[\frac{V_{ph0}}{V_{ph}(\varsigma)} - \frac{d\Phi}{d\varsigma} \right]^3 I_0\left(\frac{V_{ph0}}{V_{ph}} \rho \right) \cos\Phi - \frac{V_{ph0}}{V_{ph}^2(\varsigma)} \frac{dV_{ph}(\varsigma)}{d\varsigma} \qquad (9)$$

$$\frac{d^2\rho}{d\varsigma^2} = -\varepsilon_0 \left[\frac{V_{ph0}}{V_{ph}(\varsigma)} - \frac{d\Phi}{d\varsigma} \right]^2 \left[\frac{d\rho}{d\varsigma} I_0\left(\frac{V_{ph0}}{V_{ph}} \rho \right) \cos\Phi - I_1\left(\frac{V_{ph0}}{V_{ph}} \rho \right) \sin\Phi + \nu g(\rho) \right]$$

Here $0 \le \rho < \rho_d$, $\rho_d = k_0 r_d$, r_d- inner radius of drift tube.

$$g(\rho) = \begin{cases} \rho & \text{for } \rho < \rho_b \\ \rho_b^2 / \rho & \text{for } \rho_b < \rho \le \rho_d \end{cases}$$

In the second (beam sufficient) case ion dynamics is governed by equations set (7)-(8). The law of phase velocity changing along the resonator was chosen to satisfy the requirement of ion acceleration from initial energy $W_0=5$ MeV to final energy $W_f=8$ MeV on the resonator length $L=161$ cm.

Below the results of ion dynamics simulation will be represented taking into account these two cases.

So, further simulation of ion acceleration in EAS are based on the following main approximations.

1. During simulation we used the parameters of EAS, previously coordinated and taken to making "in hardware". (see Table 2). For generality the variation of some parameters of EAS is undertaken (current and radius of the electron beam, intensity of the accelerating field, equilibrium (synchronous) phase etc.).

Table 2. The main parameters of the Experimental Accelerating Stand (preliminary data)

1.	Input proton energy	5 Mev
2.	Output proton energy	8 MeV
3.	Proton current	30 mA
4.	Electron beam energy	350 keV
5.	Electron beam current	150 A
6.	Pulse duration	2.5 mksec
7.	Pulse frequency	1 pps
8.	Electron beam initial radius	1.3 cm
9.	Electron beam final radius	2.4 cm
10.	First drift tube radius	2.76 cm
11.	Last drift tube radius	3.5 cm
12.	Magnetic field intensity	
	for EAS input	609 Oe
	for EAS output	439 Oe
13.	Resonator length	161 cm
14.	Operating frequency	148.5 MHz
15.	Accelerating field intensity	56 kV/cm
16.	Synchronous phase	60°
17.	Shunt impedance	35 MOhms/m

2. Simulation of ion acceleration in EAS is curried out at the stage when RF-field has been already excited. The process of the RF-field excitation in H-type resonator by e-beam at ADE has been considered in our report in 1993.
3. It is supposed that e-beam is "hard" enough and relatively weakly perturbed with RF-field, so that the e-beam influence on the RF-field structure in e-beam volume can be described linearly by using of tensor of dielectric permeability $<\varepsilon_{ik}>$. The eigen frequency of the resonator is weakly disturbed by the beam ($\Delta\omega \approx 0$), see chapter 3). Nevertheless in the region, that is placed with e-beam, the RF-field radial structure can change: $I_0(k_\perp r) \rightarrow J_0(\kappa r)$.
4. Coulomb interaction of the accelerated ions on this stage did not take into account.

In the process of simulation two regimes of ions acceleration in EAS have been considered:

I. Regime of nearly whole filling of drift tubes with electron beam.
II. Regime of partial filling (approximately one half).

In each regime four cases of radial focusing of accelerated ions have been investigated.

1. Vacuum case when accelerating field in the region of the equilibrium phase defocuses the ions in radial direction and radial focusing by space charge field of e-beam is absent (accelerating field $E_z \sim E_0 I_0(k_\perp r)$; parameter, corresponding to space charge field, $\nu=0$ (see equations (5) (6)).
2. The case of radial ion focusing by direct (dc) component of space charge field of e-beam ($E_z \sim E_0 I_0(k_\perp r)$; $\nu \neq 0$).
3. The case of radial ion focusing by alternative (RF) component of excited synchronous cyclotron wave: direct component is compensated and it is not taken into account ($E_z \sim E_0 J_0(k_\perp r)$; $\nu = 0$).
4. The case of radial ion focusing both direct (dc) space charge field and alternative RF-field of excited slow wave ($E_z \sim E_0 J_0(k_\perp r)$; $\nu \neq 0$).

Procedure of simulation.

For solving of the ordinary differential equations set (7-9) Adams method of 4-th order was used [9]. The calculations were carried out for 180 particles ("ions"). At the resonator entrance they uniformly filled initial phase interval and the electron beam area (it was taken six rows on beam radius). Their initial velocity was equal to initial phase velocity $V_{ph}(0)$. Only accelerated particles were taken into account i.e. those ones which did not fall on the drift tubes sides, and did not leave phase interval $\Phi=[-1/2\pi, 3/2\pi]$.

The results of simulation.

Firstly, let us consider regime I (r_b=2.75 cm), the cases 1-4. At the resonator entrance ($z=0$) ions are uniformly distributed over the phase Φ and electron beam radius ρ_b (by six rows at radius $0 \leq \rho \leq \rho_b$). The ion phase Φ is taken from the maximum of the accelerating wave (see (3), (4)). Ions distribution are represented on the radial - phase plane (r, Φ) at z=40; 80; 120; 160 cm. (The value z=160 cm corresponds to the resonator exit; the dimensionless radius: $\rho=k_0 r$, where k_0=0.3 cm^{-1}). Fig.5a, b corresponds to the case I.1, i.e. to absence of ion radial focusing. Accelerating wave amplitude E_0 is equal to 56 kV/cm (5a), and 100 kV/cm (5b). (Accelerating rate T for the middle area of the EAS is equal to 28 keV/cm: $T=eE_0\cos\Phi_s$, where Φ_s is the synchronous phase). Strong radial defocusing have place near $\Phi=\pi/2$ (where E_r have a maximum value), already for z=40 cm. At the accelerator's exit a relative amount of accelerated ions ($\eta=N_{acc.}/N_{inject.}$) not exceed 20 % (generally, there are ions going along the axis where E_r=0). Fig.6a, b corresponds to the case I.2, i.e. to ion radial focusing by dc component of Coulomb field of an electron beam with current values of 150 A (6a), and 300 A (6b). In this case this type of focusing is not efficient because drift tubes' walls are placed too close to beam boundary. For E_0=56 kV/cm and I_e=150 A $\rightarrow \eta$=0.2; I_e=300 A $\rightarrow \eta$=0.3; I_e=600 A $\rightarrow \eta$=0.45.

In Fig.7a, b it is represented the case I.3 which corresponds to RF focusing by an accelerated field. In this case good ion focusing has place: for E_0=56 kV/cm → η=0.50 (7a), and for E_0=100 kV/cm → η=0.59 (7b).

Fig.8a, b corresponds to the case I.4 where ion focusing is realized simultaneously by dc and ac (RF-) components of space charge of an electron beam. For E_0=56 kV/cm and beam current I_e=150 A → η=0.54 (8a). For E_0=100 kV/cm, and I_e=150 A → η=0.67 (8b). In comparison with the case I.3, it is followed that RF focusing is more sufficient in this regime.

Let us investigate now the regime II (for r_b=1.3 cm), cases 1-4.

In Fig.9a, b the case II.1 is represented. Now beam boundary is not close to drift tubes' walls, and some ions can be accelerated without focusing: for E_0=56 kV/cm → η=0.31 (9a), for E_0=100 kV/cm → η=0.26 (9b).

Fig.10a, b corresponds to the case II.2 for E_0=56 kV/cm, and I_e=150 A (10a); 300 A (10b). For these parameters Coulomb forces provide good radial focusing (η=0.61). Following the simulation results one can compile a Table 3.

Table 3

E_0=56 kV/cm

I_e (A)	50	100	150	300	600
η	0.4	0.53	0.61	0.61	0.61

E_0=100 kV/cm

I_e (A)	50	100	150	300
η	0.29	0.34	0.4	0.68

E_0=200 kV/cm

I_e (A)	50	100	150	300	600
η	0.25	0.25	0.28	0.35	0.73

Note that saturation of η have place at $I_e \approx 3E_0$, where I_e in Amperes, and E_0 in kV/cm.

As we can see in Fig.11a, b, we have good ion RF focusing for the case II.3 also. For E_0=56 kV/cm → η=0.59 (11a), and for E_0=100 kV/cm → η=0.66 (11b).

In Fig.12a, b it is represented results for the case II.4 at beam current I_e=150 A, and E_0=56 kV/cm (12a), E_0=100 kV/cm (12b). Then η=0.62 (12a), and η=0.72 (12b).

As it follows from all these data, full ion radial focusing is provided for EAS parameters E_0=56 kV/cm, I_e=150 A in cases II.2-II.4. In case II.4 the least ion beam radius is achieved: ρ_i=0.2-0.3, or r_i=0.6-0.9 cm.

Let us also adduce the simulation results for relatively small fields: E_0=30 kV/cm, φ_s=21°, and E_0=40 kV/cm, φ_s=46° (see Table 4).

Table 4

E_0=30 kV/cm. Case II.1; η=0.33: ρ_i=1.08

Case II.2.

I_e (A)	30	50	100
η	0.39	0.39	0.39
ρ_i	1.08	0.75	0.40

Case II.3: η=0.42

Case II.4.

I_e (A)	30	50	100
η	0.42	0.42	0.42
ρ_i	0.55	0.55	0.41

E_0=40 kV/cm. Case II.1: η=0.33; ρ_i=1.10

Case II.2.

I_e (A)	40	80	120	150
η	0.44	0.51	0.51	0.51
ρ_i	1.10	0.50	0.50	0.41

Case II.3: η=0.52

Case II.4.

I_e (A)	40	80	120	150
η	0.52	0.52	0.52	0.52
ρ_i	0.61	0.50	0.40	0.38

As it follows from these data, for these fields ions can be accelerated in EAS even without radial focusing. Radial focusing lead to radial compression of ion beam (see cases II.2, II.4).

To determine ion beam emittance $\mathcal{E}$ sets of imaging (representing) points in $\left(r, \dot{r}/\beta_{ph}\right)$ coordinates were obtained for all above - mentioned cases and parameters. Generally, we have interest to main EAS parameters.

In Fig.13a it is represented a set of imaging points in the wave frame for E_0=56 kV/cm, I_e=150 A, r_b=1.3 cm, in case of ion focusing by dc component of electron beam space charge (case II.2). In this case the value of emittance (in the wave frame) is $\mathcal{E} \equiv \pi \cdot 0.039$ (cm·rad).

In Fig.13b it is represented a set of imaging points for E_0=56 kV/cm, I_e=150 A, r_b=1.3 cm, in case of ion focusing by dc and RF components of electron beam space charge (case II.4). In this case $\mathcal{E} \equiv \pi \cdot 0.019$ (cm·rad).

Let us note that in case of Fig.13b one can see an ordered arrangement of imaging points which better can be seen in next Fig.13c (for parameters E_0=200 kV/cm, I_e=150 A, case II.4). It is seen that imaging points not occupy all area of the ellipse with its semi-axes ρ=0.3, $\dot{\rho}/\beta_{ph} = 0.4$, but they are arranged along five ellipse curves (it is corresponds to garmonic oscillations of ions due to focusing process). In this case a real emittance is sufficiently less than effective one [16] determined by standard method for the external ellipse.

In Fig.13d it is represented a set of imaging points for case II.1 (without focusing) at E_0=56 kV/cm. The imaging points are placed along a straight line going out of the origin of coordinates while the defocusing force $F_r = |e/E_r$ is proportional to the radial coordinate. One can see a few imaging points with $\dot{r} < 0$ corresponding to ions moving to the axis.

By simulation one can determine a velocity spectrum $N(V_i)$ of accelerated ions. In Fig.14a, b, c this spectrum is represented in $\left(N, \dot{\Phi}\right)$ coordinates for the resonator exit. The spectrum of Fig.14a corresponds to the conditions of Fig.9a (E_0=56 kV/cm, without focusing). The spectrum of Fig.14b corresponds to Fig.10a (E_0=56 kV/cm, I_e=150 A, focusing by dc component of electron beam space charge). The spectrum of Fig.14c corresponds to Fig.12a (E_0=56 kV/cm, I_e=150 A, focusing by both dc and RF components of electron beam space charge).

From the expression for the phase of an ion in the accelerating wave we have:

$$\frac{d\Phi}{dz} = k_0 \frac{d\Phi}{d\varsigma} = \omega\left[\frac{1}{V_{ph}} - \frac{1}{V_i(z)}\right] \tag{10}$$

where $V_i(z)$ is the ion velocity in the laboratory frame.

From (10) one can obtain the expression for the velocity spread of accelerated ions:

$$\Delta V_i = V_{i\max} - V_{i\min} = \left[\frac{1}{V_{ph}(L)} - \frac{1}{V_{ph0}}\frac{d\Phi}{d\varsigma}\bigg|_{\max}\right]^{-1} - \left[\frac{1}{V_{ph}(L)} - \frac{1}{V_{ph0}}\frac{d\Phi}{d\varsigma}\bigg|_{\min}\right]^{-1} \tag{11}$$

For data represented by Fig.14 we have:

$$\frac{\Delta V_i}{V_{ph}} = \frac{\Delta V_i}{V_{i,syn}} \cong 0.16$$

There is relatively big value of the ions velocity spread. It is explained by sufficient amplitudes of phase oscillations of accelerated ions.

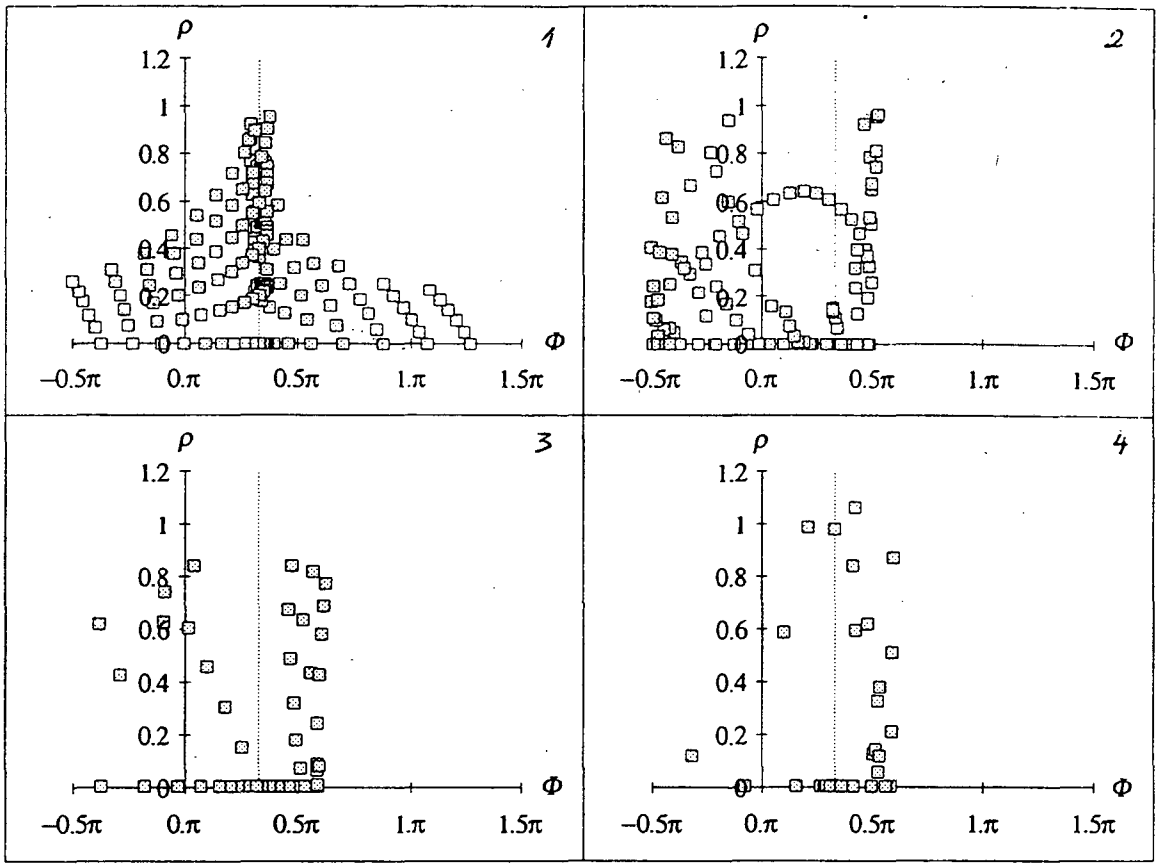
ρ
1
1.2
1
0.8
0.6
0.4
0.2
0
Φ
−0.5π
0.π
0.5π
1.π
1.5π
ρ
2
1.2
1
0.8
0.6
0.4
0.2
0
Φ
−0.5π
0.π
0.5π
1.π
1.5π
ρ
3
1.2
1
0.8
0.6
0.4
0.2
0
Φ
−0.5π
0.π
0.5π
1.π
1.5π
ρ
4
1.2
1
0.8
0.6
0.4
0.2
0
Φ
−0.5π
0.π
0.5π
1.π
1.5π

Fig.5a

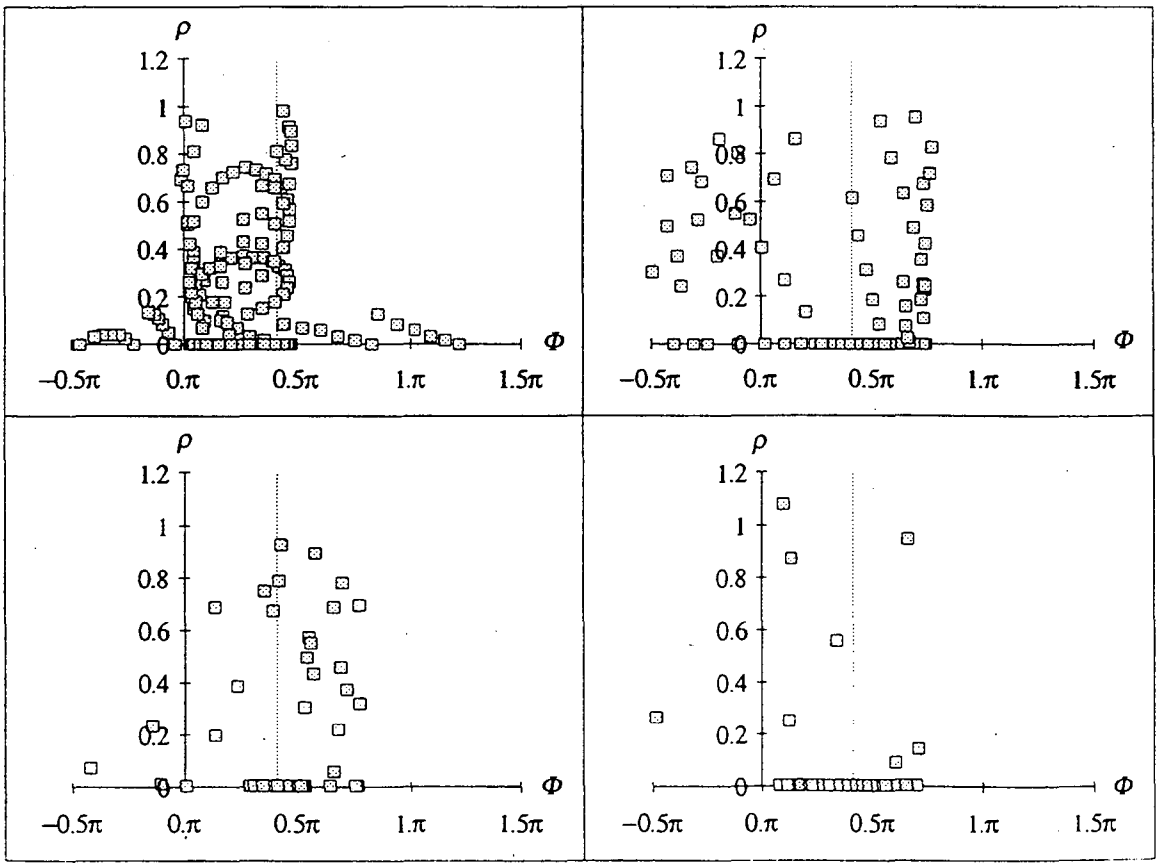
ρ
1.2
1
0.8
0.6
0.4
0.2
0
Φ
−0.5π
0.π
0.5π
1.π
1.5π
ρ
1.2
1
0.8
0.6
0.4
0.2
0
Φ
−0.5π
0.π
0.5π
1.π
1.5π
ρ
1.2
1
0.8
0.6
0.4
0.2
0
Φ
−0.5π
0.π
0.5π
1.π
1.5π
ρ
1.2
1
0.8
0.6
0.4
0.2
0
Φ
−0.5π
0.π
0.5π
1.π
1.5π

Fig.5b

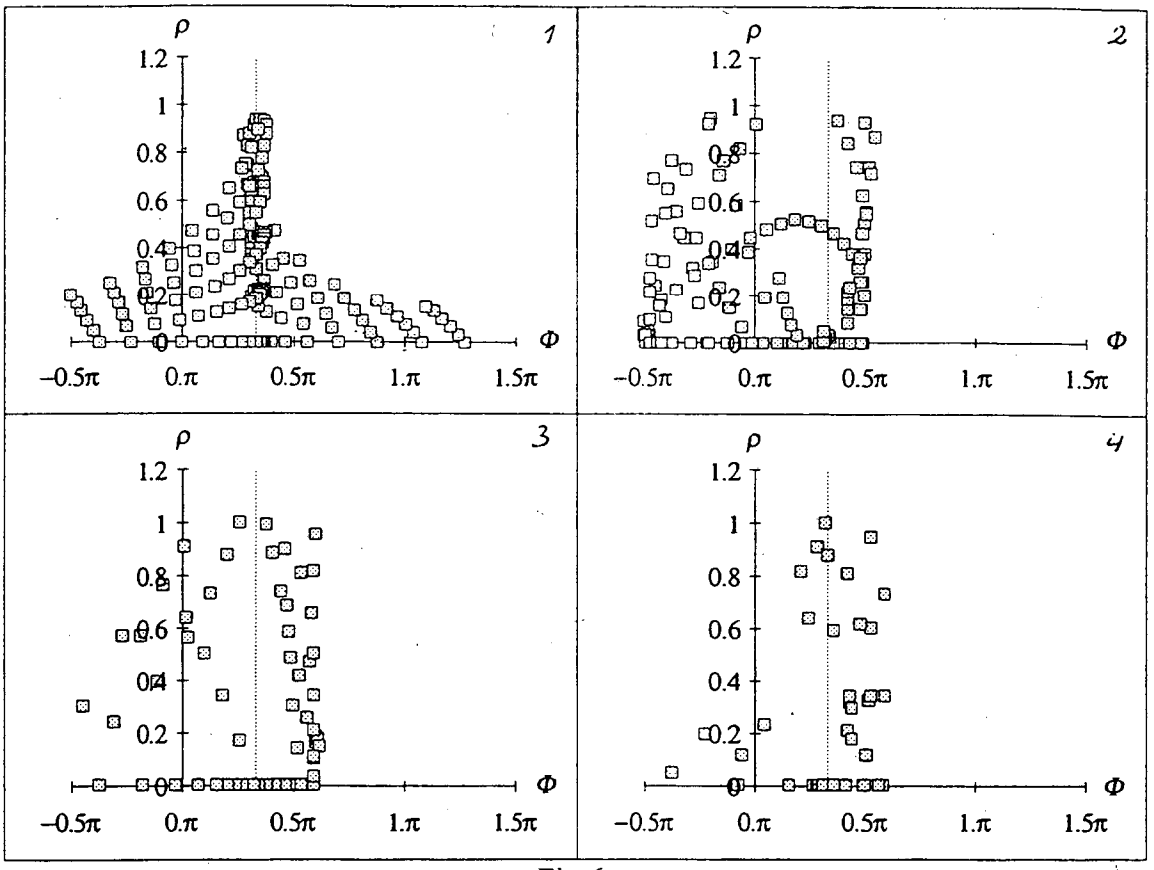
ρ
1
2
3
4
1.2
1
0.8
0.6
0.4
0.2
0
Φ
−0.5π
0.π
0.5π
1.π
1.5π

Fig.6a

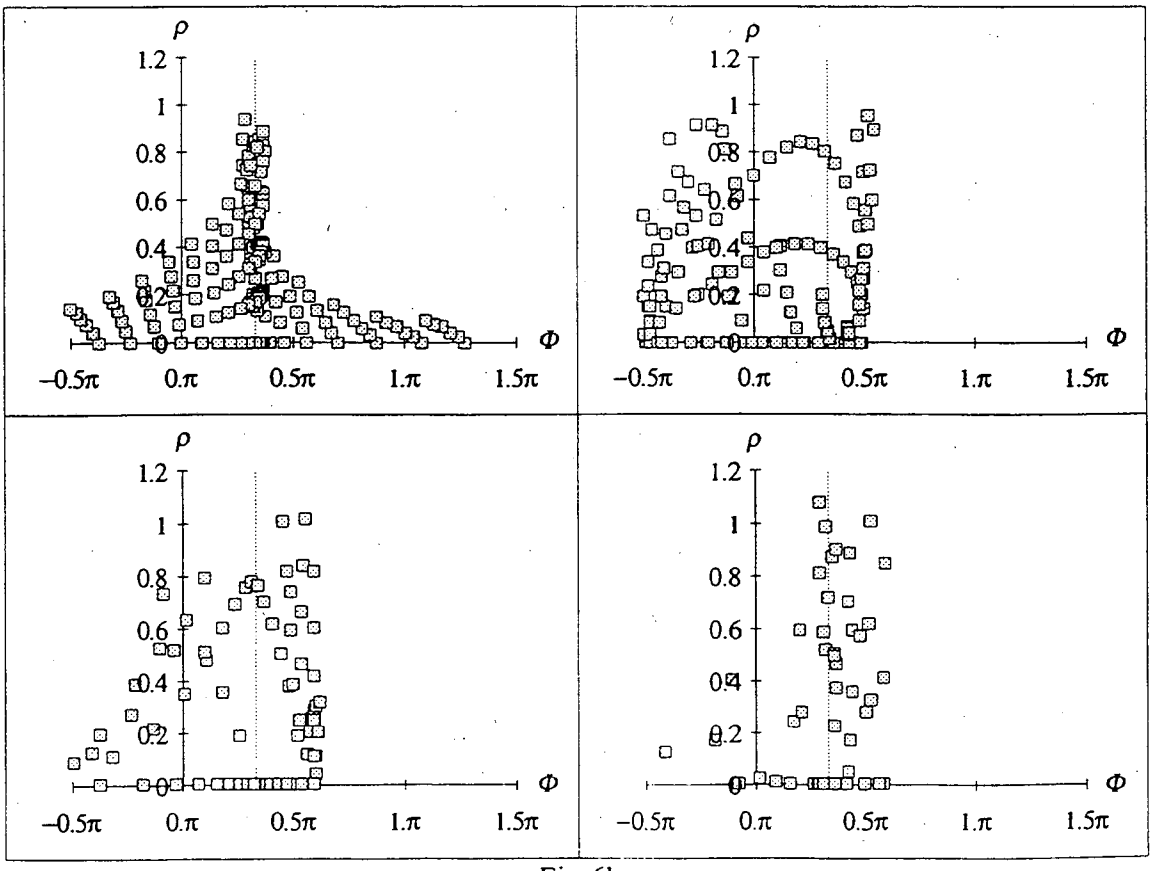
ρ
1.2
1
0.8
0.6
0.4
0.2
0
Φ
−0.5π
0.π
0.5π
1.π
1.5π

Fig.6b

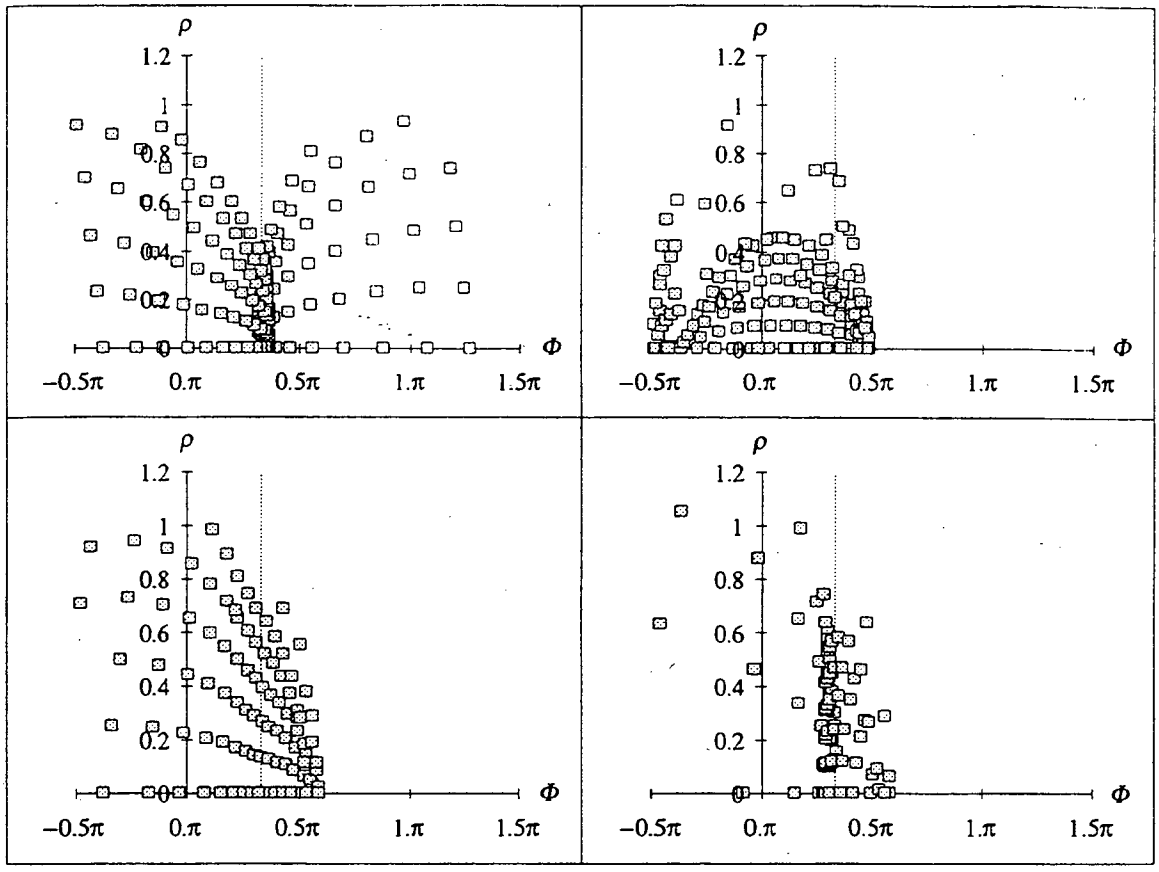
ρ
Φ
1.2
1
0.8
0.6
0.4
0.2
0
−0.5π
0.π
0.5π
1.π
1.5π

Fig.7a

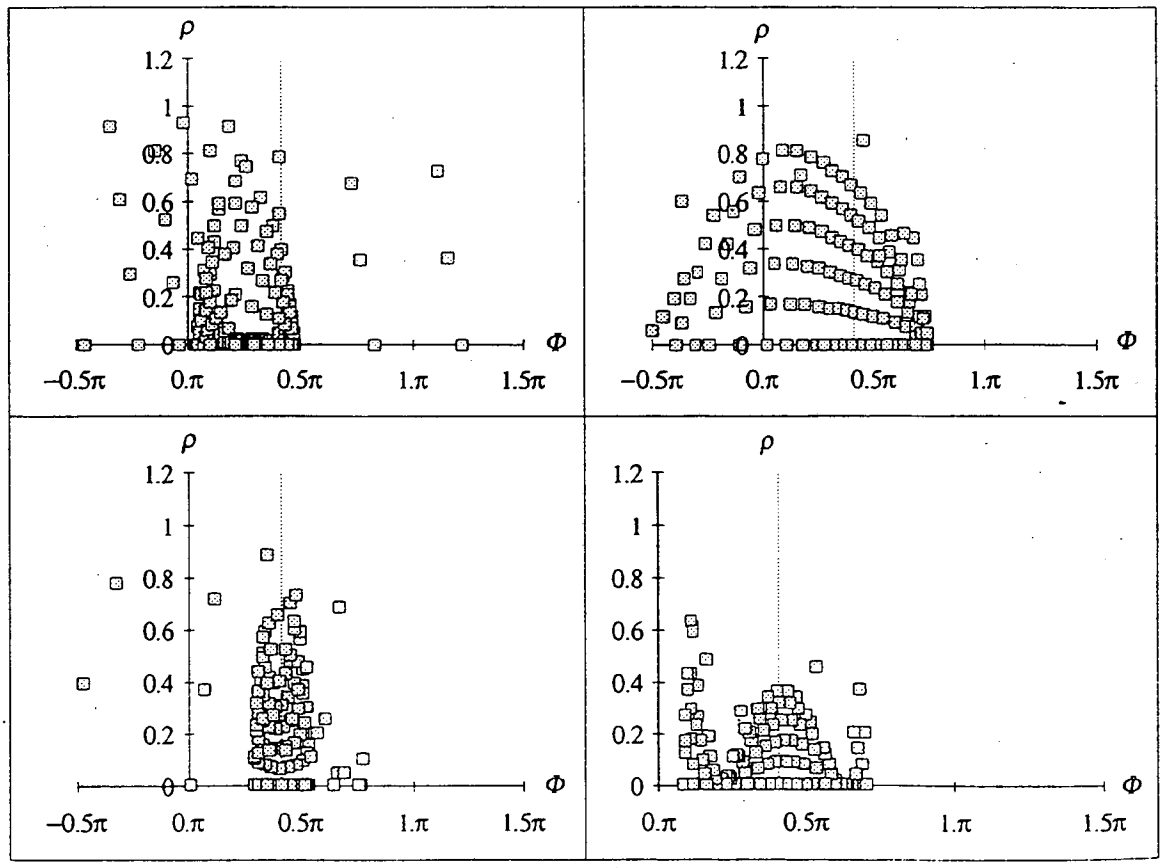
ρ
Φ
1.2
1
0.8
0.6
0.4
0.2
0
−0.5π
0.π
0.5π
1.π
1.5π

Fig.7b

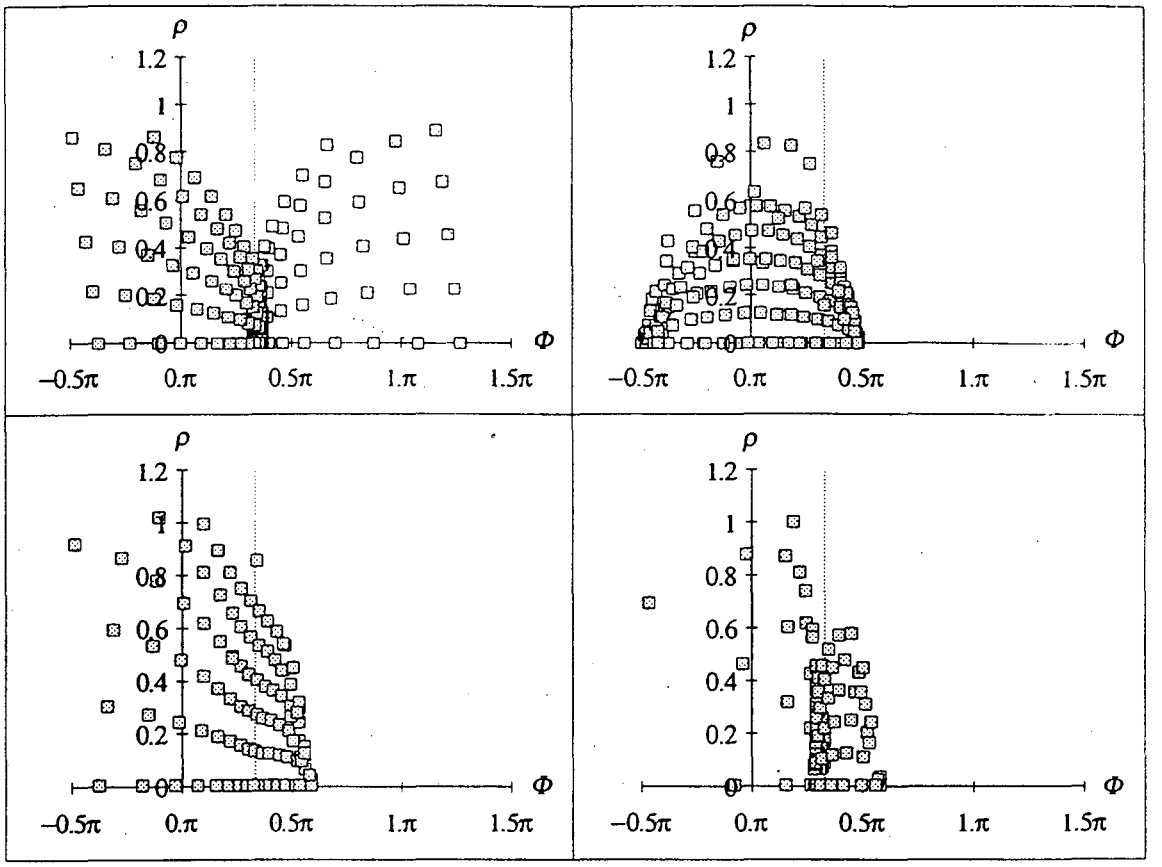
ρ
Φ
1.2
1
0.8
0.6
0.4
0.2
0
–0.5π
0.π
0.5π
1.π
1.5π

Fig.8a

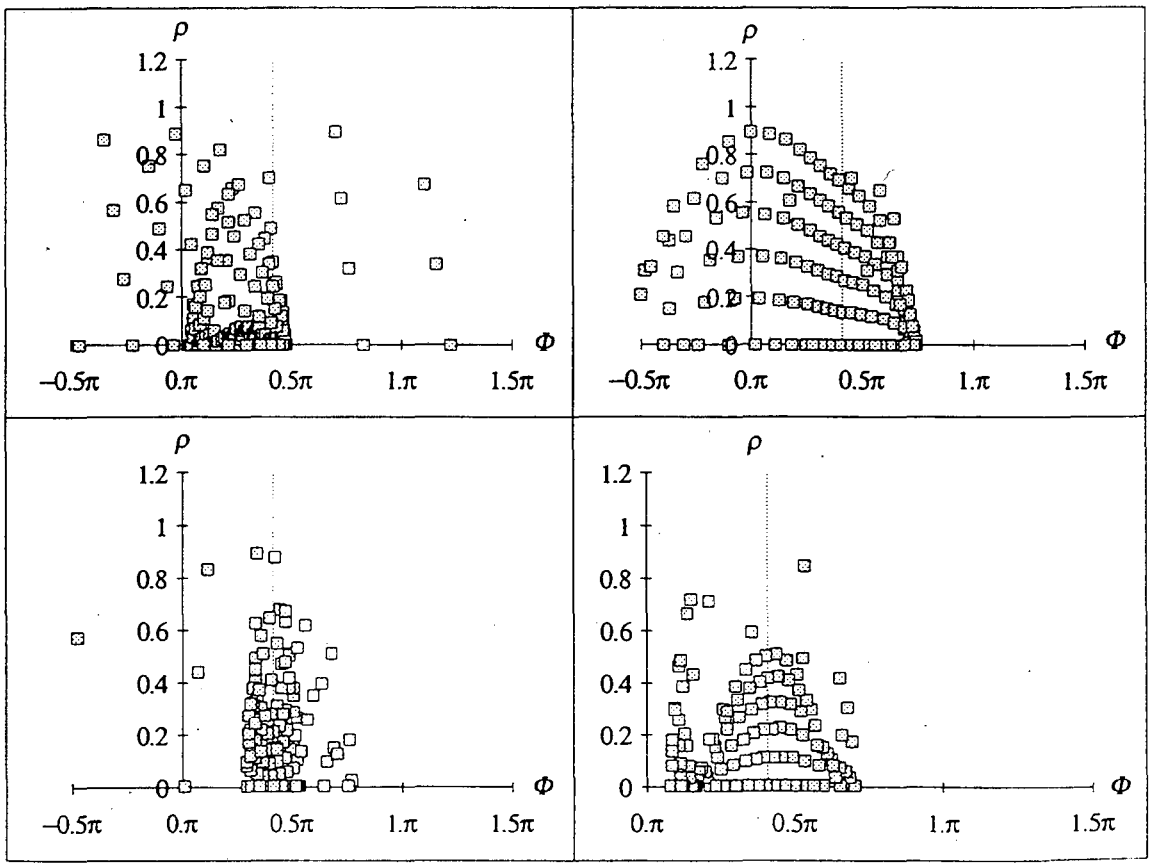
ρ
Φ
1.2
1
0.8
0.6
0.4
0.2
0
–0.5π
0.π
0.5π
1.π
1.5π

Fig.8b

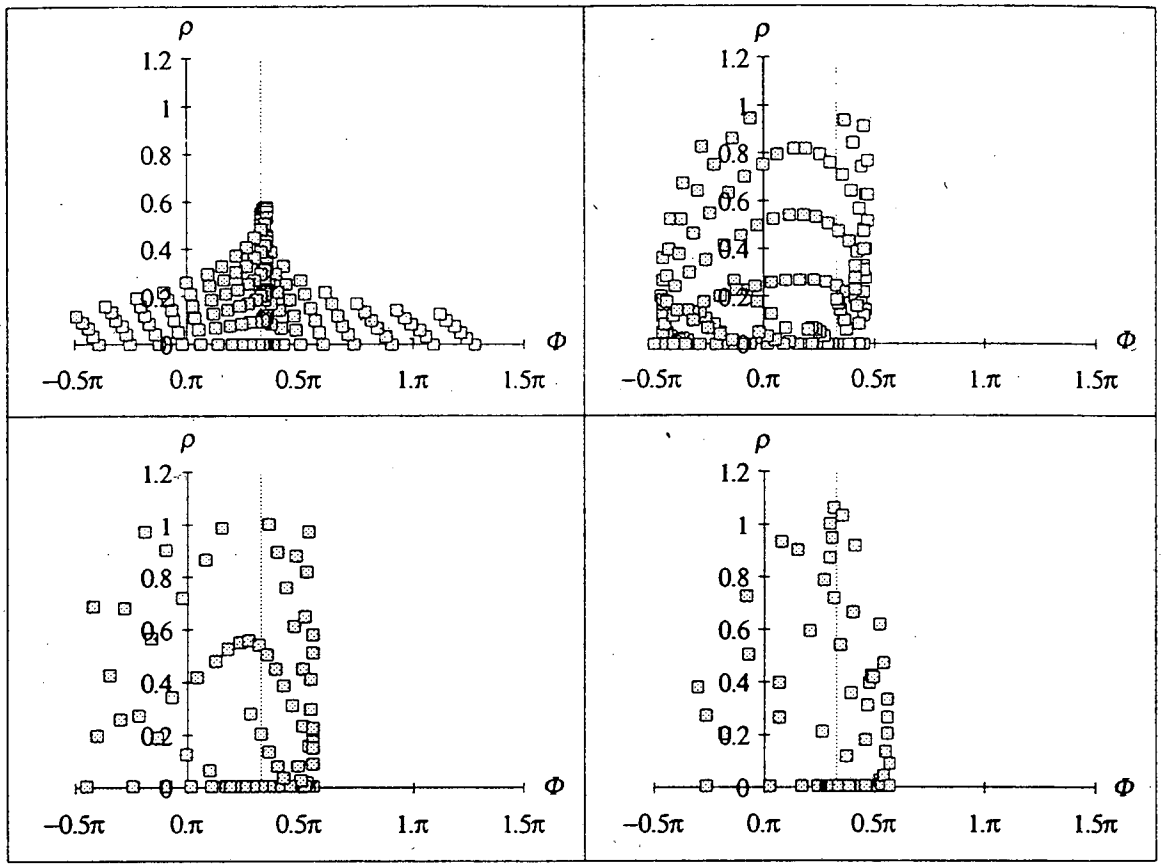
ρ
1.2
1
0.8
0.6
0.4
0.2
0
Φ
−0.5π
0.π
0.5π
1.π
1.5π

Fig.9a

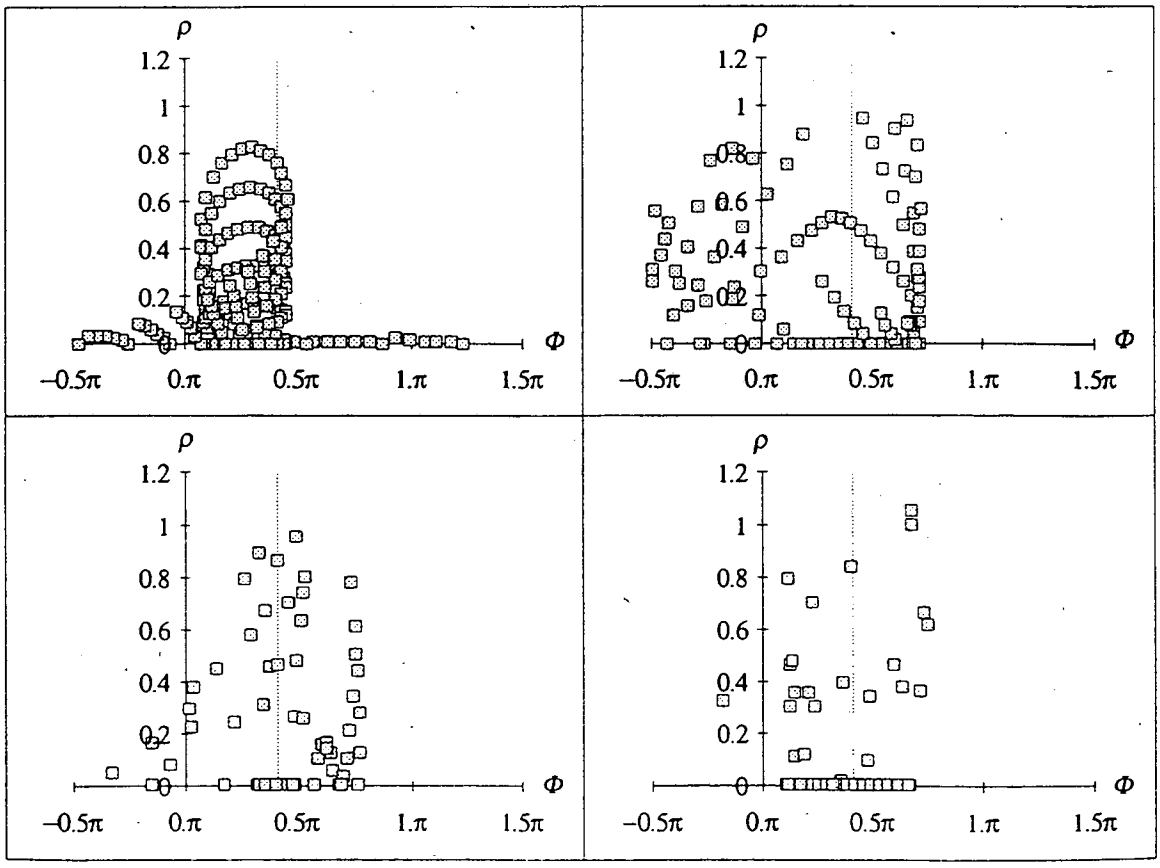
ρ
1.2
1
0.8
0.6
0.4
0.2
0
Φ
−0.5π
0.π
0.5π
1.π
1.5π

Fig.9b

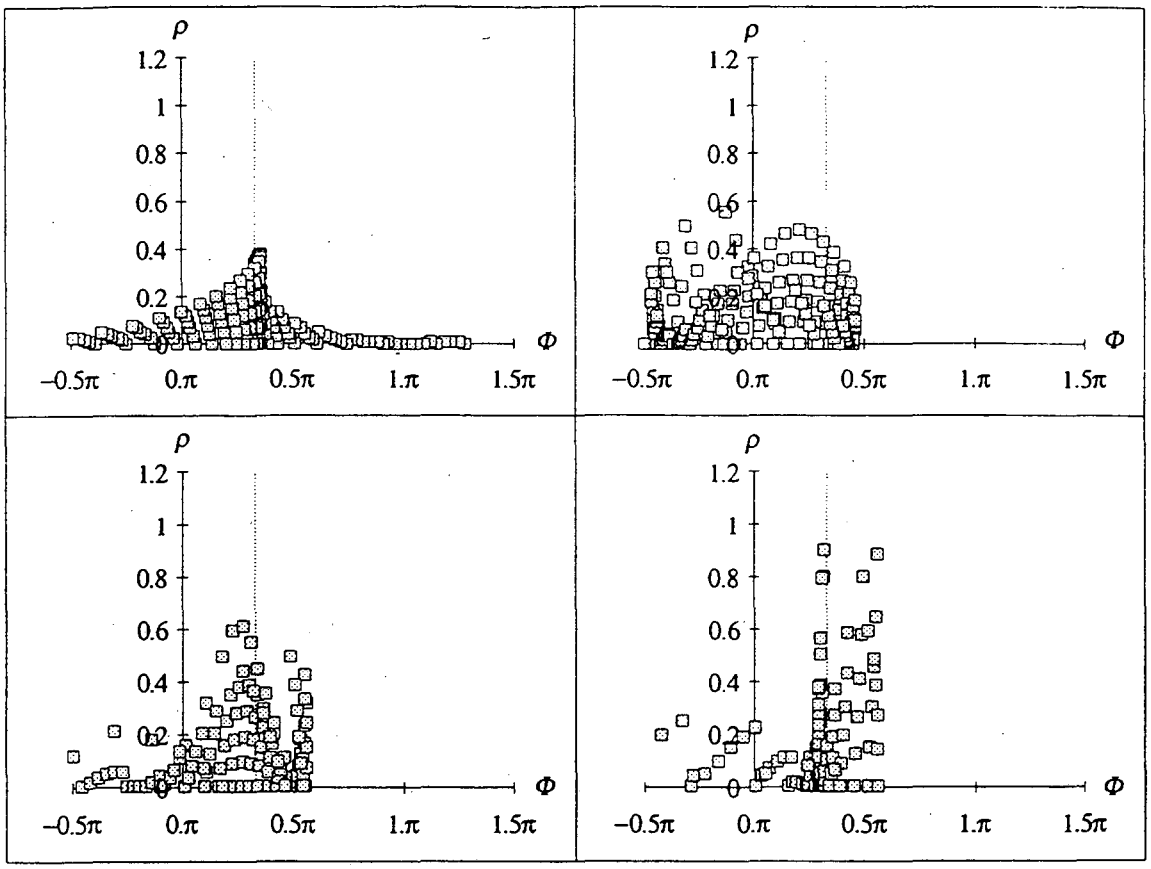

Fig.10a

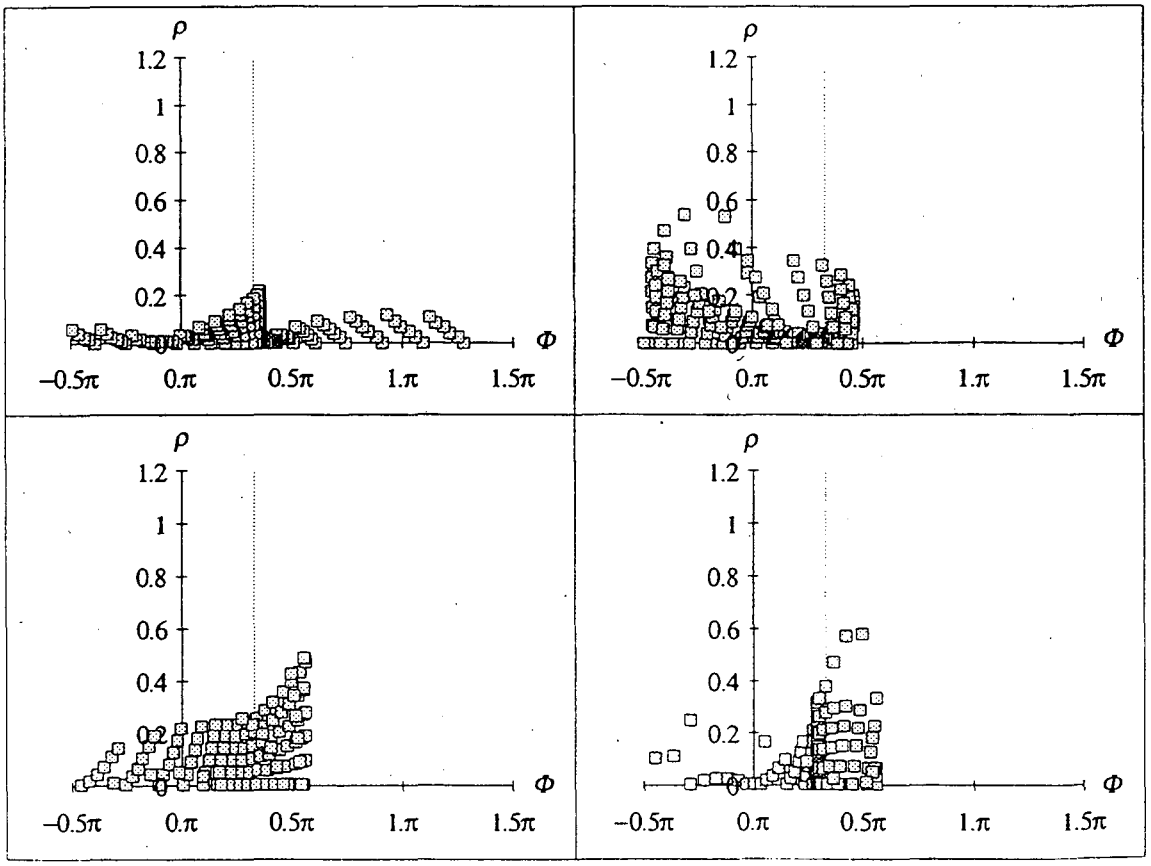

Fig.10b

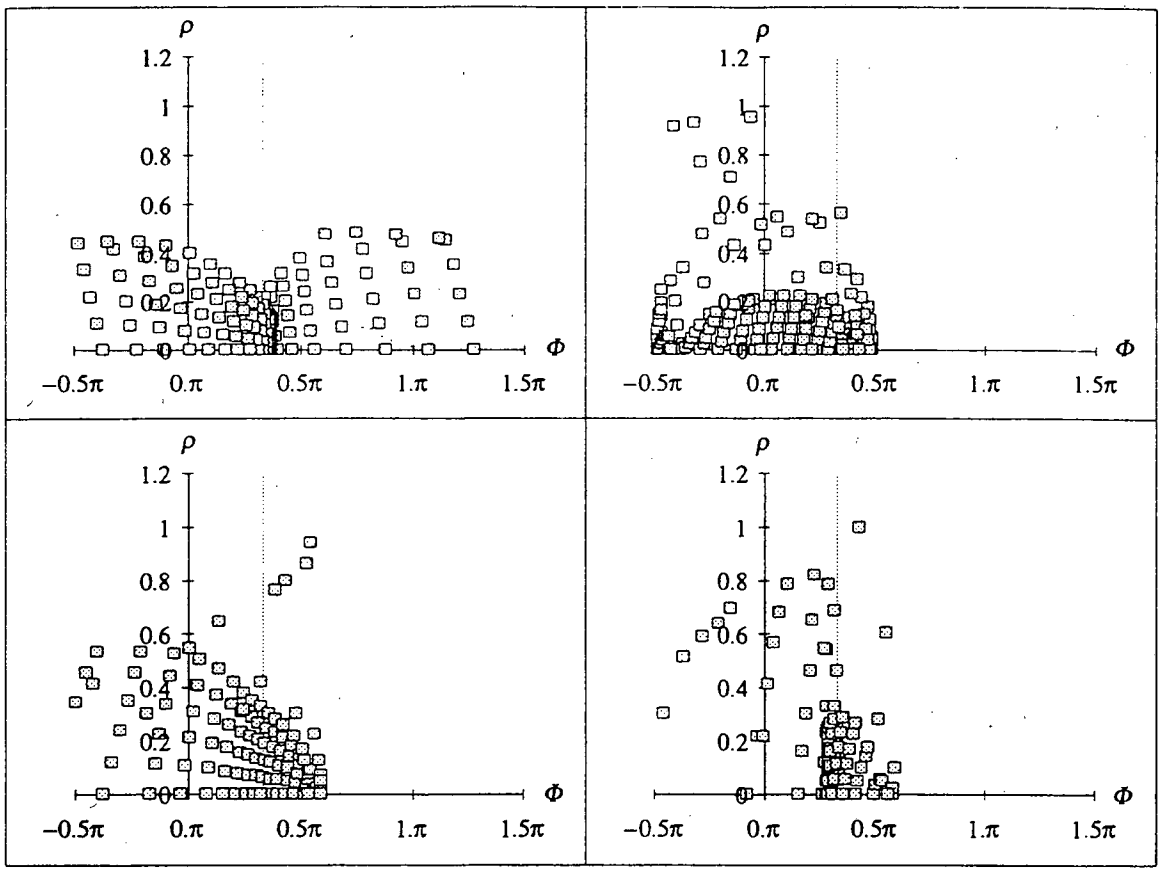

Fig.11a

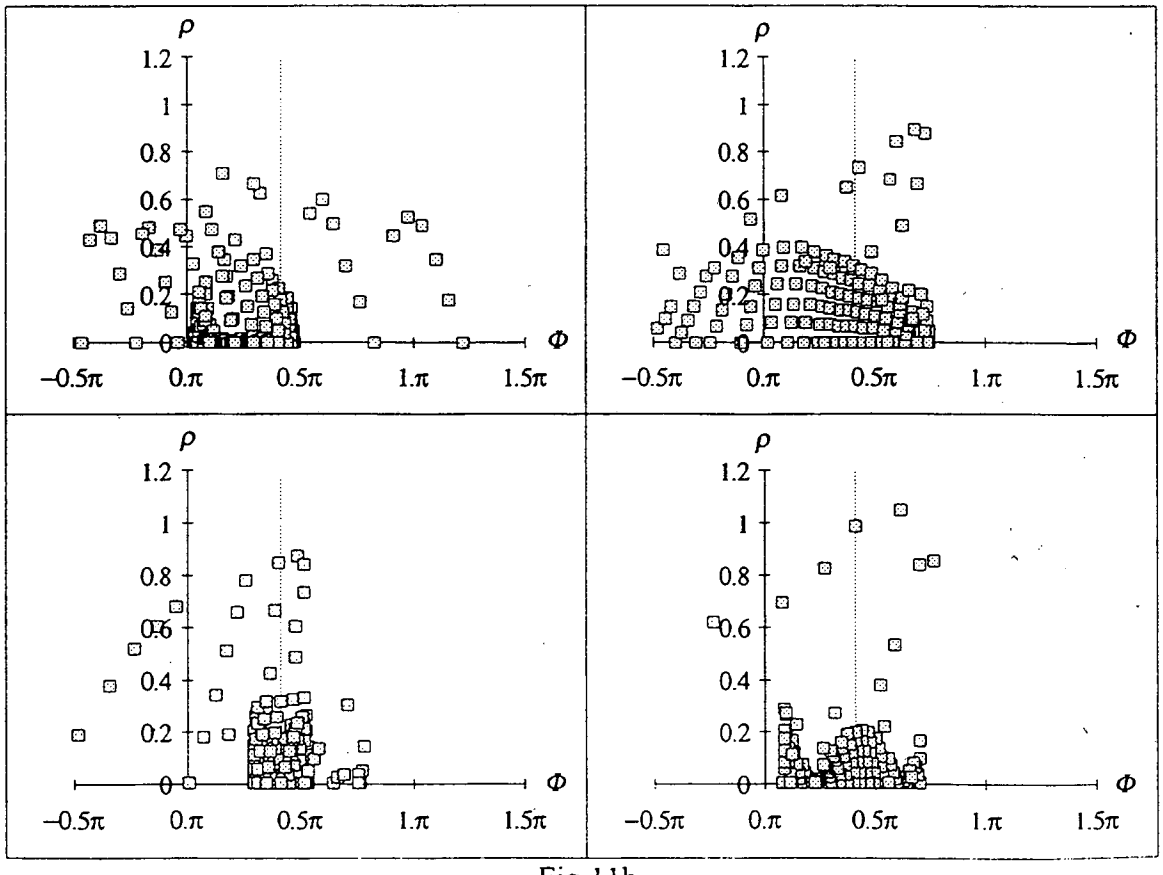

Fig.11b

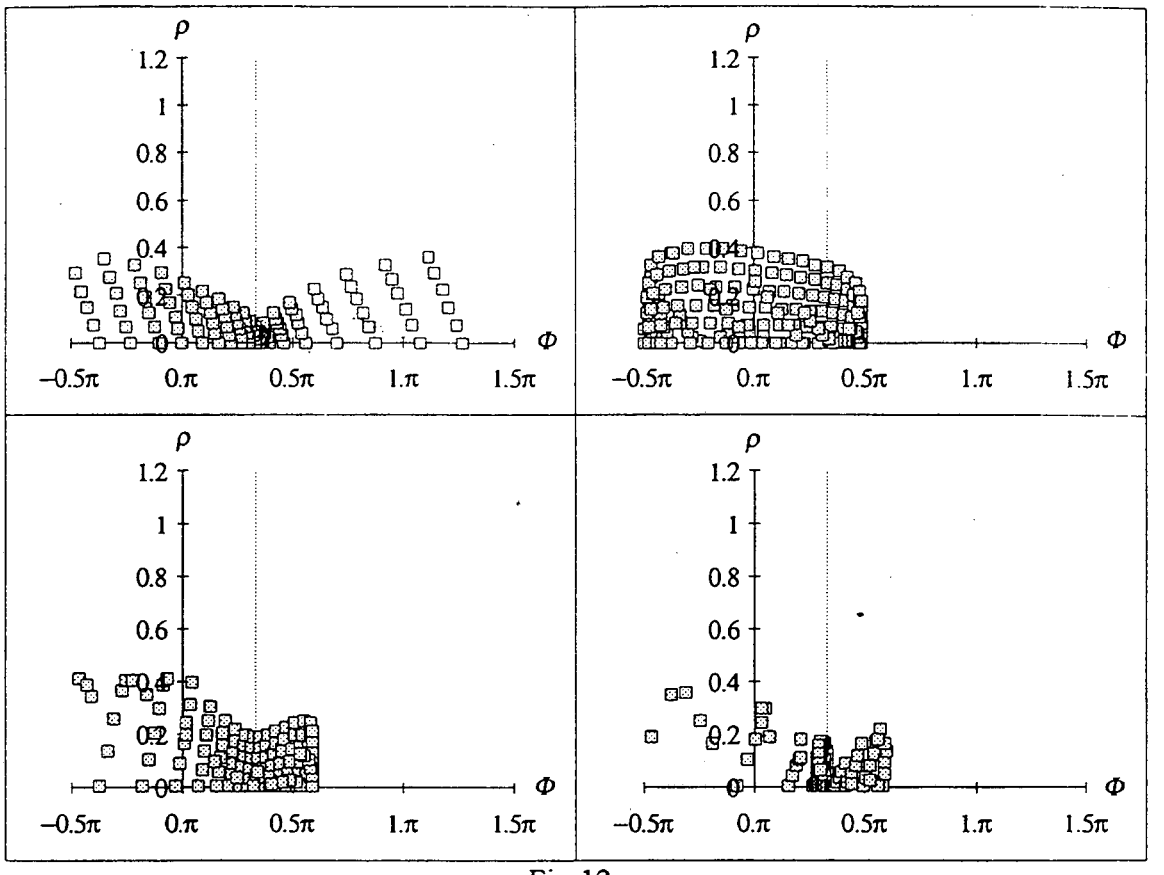

Fig.12a

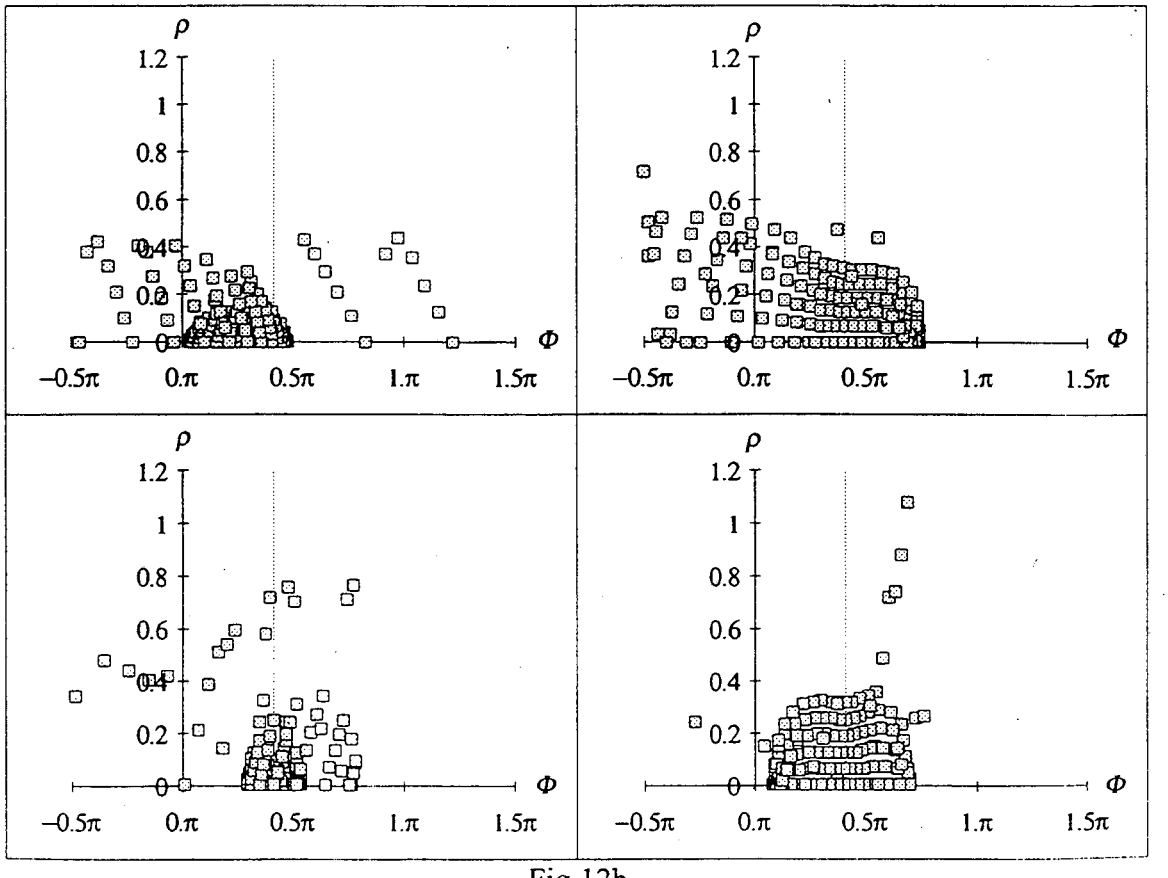

Fig.12b

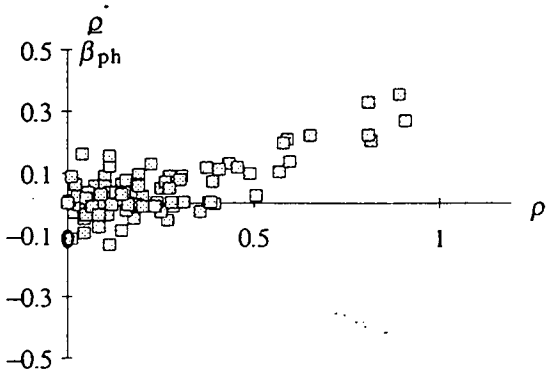

Fig.13a

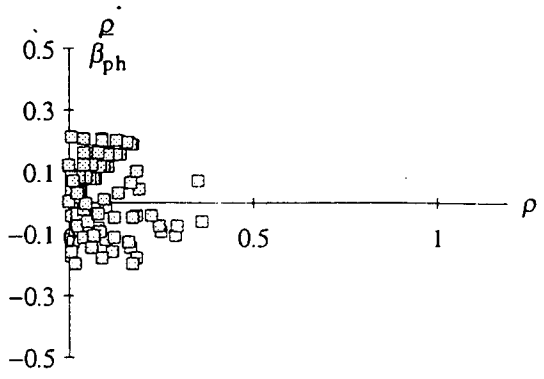

Fig.13b

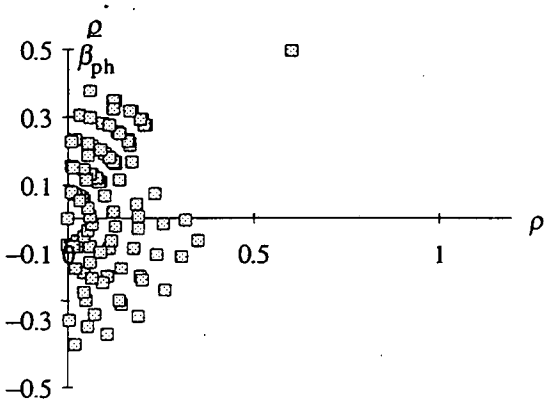

Fig.13c

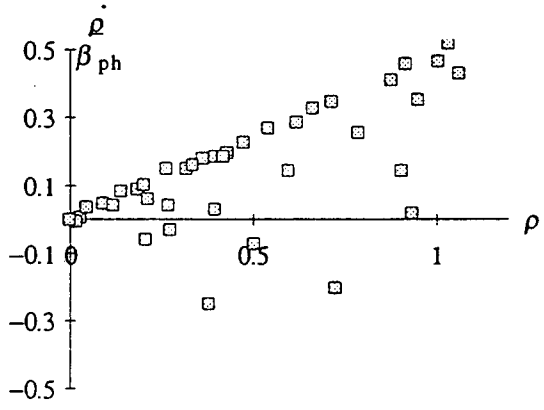

Fig.13d

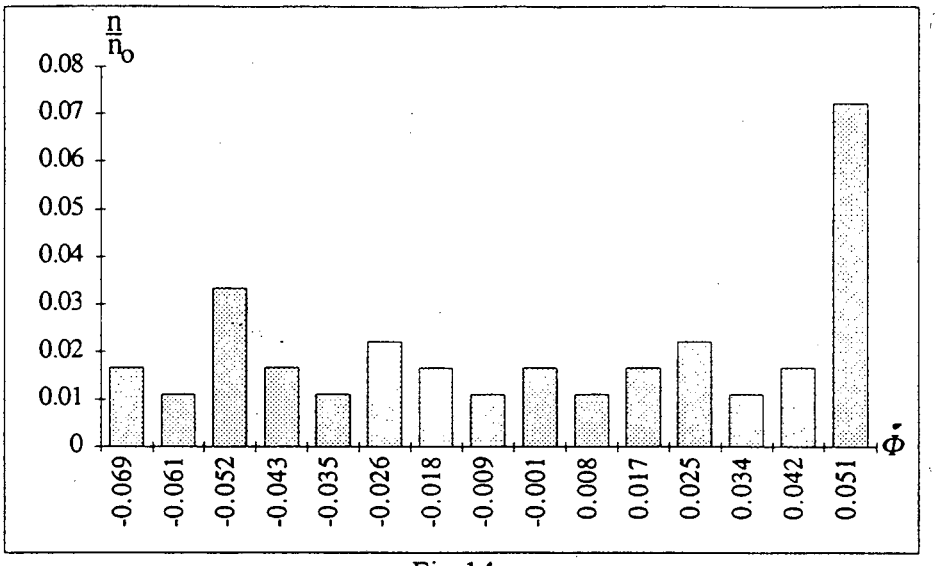

Fig.14a

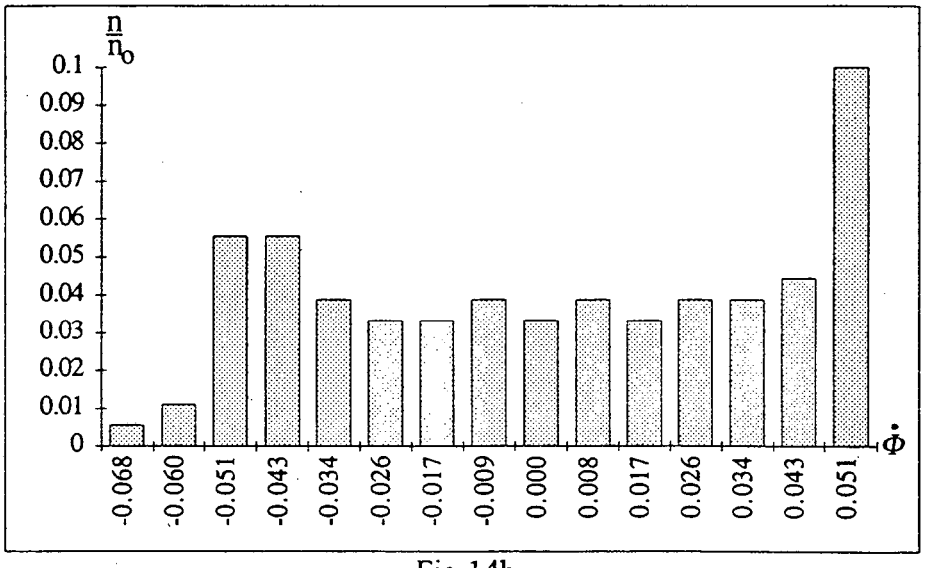

Fig.14b

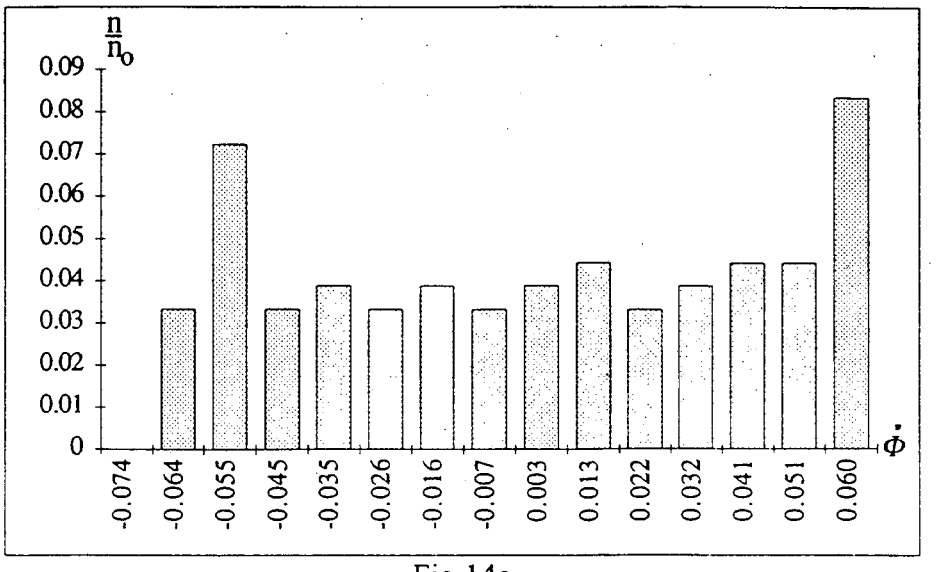

Fig.14c

6. Summary

In this Report are presented the results of the second stage of the project "Development of a two-beam high-current ion accelerator based on Doppler effect". In accordance with Purchase Order No. 4596310 the work is fulfilled including the following items:

I. Start of the manufacture of the Experimental Accelerating Stand (EAS) - the section for proton acceleration from 5 MeV to 8 MeV, in which RF fields are excited by an electron beam at the anomalous Doppler effect.

II. Theoretical investigation and computer simulation of field excitation and ion acceleration in the EAS.

The following results are obtained.

1. Under item I, the EAS manufacturing is begun. To present time, a pedestal for the EAS and a stainless steel vacuum chamber for RF resonator have been made. Besides, parts (workpieces) of the EAS RF resonator with the acceleration structure have been manufactured, and its assembly is begun.
2. Under item II, it is realized three works: calculation of frequency shift and increment for the EAS resonator exciting due to anomalous Doppler effect in a non-uniform case; calculation of the EAS solenoid for creation of magnetic field with a required spatial distribution; theoretical investigations and computer simulations of ion acceleration in a two-beam electron-ion accelerator (with regarding the main EAS parameters).
3. In area of the cyclotron resonance under anomalous Doppler effect it have been determined the conditions favorable for analysis and functioning of a two-beam ion accelerator (in particularly, the EAS), when RF fields are excited at zero shift of resonator frequency. It have been determined the values of the start current, the RF oscillations excitation increment, the frequency shift of the H-type resonator for the main EAS parameters.
4. The method of stationary magnetic field synthesis with required dependence on longitudinal coordinate is described. Thus it is used the regularization method developed by Acad. A.N. Tikhonov for solution of (so named) incorrect inverse problems. By this method the calculation of a solenoid for creation of a non-uniform resonant magnetic field in the EAS is accomplished. In this case the conditions of resonance under anomalous Doppler effect is fulfilled on all length of the EAS resonator in spite of the fact that the phase velocity of accelerating wave changes along the EAS.
5. The results of theoretical investigations and computer simulations of ion acceleration in a two-beam electron-ion accelerator are represented (with taking into account of the main EAS parameters). Detailed studies of ion acceleration dynamics and its radial focusing have been realized. Computer simulations of ion acceleration and focusing have been accomplished for wide set of parameters including the main EAS parameters.
6. The investigations carried out show this acceleration method to advantage, and lead to expediency of a research and development continuation.

In this Report Drs. B.I. Ivanov, V.I. Butenko, M.I. Kapchinsky, V.V Ognivenko, I.N. Onishchenko, V.P. Prishchepov have taken part.

References

1. Kapchinsky M.I., Yudin L.A. Modernization of Perturbation Method for Investigation of Beam-Cavity Interaction. Izv. Vys. Uch. Zav., Ser. Radiophysics, 1990, V. 33, No 7, P. 832-840.
2. Dobranos I.A., Gorozhanin D.V., Ivanov B.I., Kapchinsky M.I. Theoretical and Experimental Investigation of H-type Resonator Reaction Upon Loading It by Electron Beam. Radiotechnics and Electronics. 1991, V. 36, No 7, P. 1309-1315.
3. Kapchinsky M.I., Yudin L.A. Electron Beam Instability in a Waveguide With Focusing by Periodical Axe-Symmetrical Field. Journ. Techn. Physics. 1991, V. 61, No 3, P. 99-107.
4. Tikhonov A.N., Arsenin V.Ya. The Methods of Solutions of Incorrect Problems. M.: Nauka, 1986.
5. Kapitsa S.P. In: " Electronics of Large Powers". M.: Nauka, 1963. No 2. P. 109-118.
6. Grabar' L.P. In: "Electronics of Large Powers". M.: Nauka, 1968. No 5. P. 195-208.
7. Adamiak K. Appl. Phys. 1978. Vol. 16. No 4. P. 417-423.
8. Lugansky L.B. Journ. Techn. Phys. 1985. V. 55. No. 7. P. 1263-1265.
9. Korn G., Korn T. Mathematical Handbook for Scientists and Engineers. McGrow-Hill Book Comp. 1968.
10. Goncharsky A.V., Leonov A.S., Yagola A.G. DAN USSR. 1974. V. 214. No 3. P. 499-500.
11. Butenko V.I. Journ. Techn. Phys. 1992. V.62. No. 7. P. 157.
12. Kapchinsky I.M. Theory of Linear Resonance Accelerators. Moscow, Energoizdat, 1982.
13. Indykul V.P., Panchenko I.P., Shapiro V.D., Shevchenko V.I. Plasma Phys., V.2, No.5, P. 775 (1976).
14. Ivanov B.I., Onishchenko I.N., Podobinsky V.O. Problems of Atomic Sciences and Techn. - Techn. of Phys. Exper., No.1(27), P. 75-77 (1986). (In Russian).
15. Kapchinsky M.I., Onishchenko I.N., Panchenko I.P. Journ. Techn. Phys. V.56, No.2. P. 263-268 (1986).
16. Banford A.P. The Transport of Charged Particle Beams, London, 1966.

LAWRENCE BERKELEY LABORATORY
UNIVERSITY OF CALIFORNIA
TECHNICAL AND ELECTRONIC
INFORMATION DEPARTMENT
BERKELEY, CALIFORNIA 94720